

Chapter 12

Windy Craggy, Northwestern British Columbia:
The World's Largest Besshi-Type Deposit

JAN M. PETER

Mineral Resources Division, Geological Survey of Canada, 601 Booth St., Ottawa, Ontario, Canada K1A 0E8

AND STEVEN D. SCOTT

Marine Geology Research Laboratory, Department of Geology, University of Toronto, 22 Russell St., Toronto, Ontario, Canada M5S 3B1

Introduction

In the geological record there exists a group of massive sulfide deposits that have been termed "Besshi-type" for their resemblance to the late Paleozoic massive sulfides at the Besshi mine on Shikoku Island, Japan (e.g., Slack, 1993). Besshi-type deposits are characterized by conformable, stratiform, blanket-like sheets of massive pyrrhotite and/or pyrite with variable contents of chalcopyrite, minor sphalerite, and rare galena. Copper is the principal economic metal, and there is subordinate zinc, cobalt, silver, and/or gold. The ores occur in submarine mafic volcanic rocks and associated marine sedimentary rocks including metagraywacke, quartzite, and metapelite that are mostly of deep-water facies. Felsic meta-igneous rocks are rare to absent, and mafic meta-igneous rocks generally are volumetrically subordinate to sedimentary rocks, although in some deposits the former predominate. Besshi-type deposits may form in numerous tectonic settings including back arc basins, rifted continental margins, intracontinental rifts, fore arcs, and sedimented spreading ridges proximal to continental land masses. The sheet-like or tabular morphology of many Besshi-type deposits is due to post-depositional deformation.

The Windy Craggy Cu-Co-Au massive sulfide deposit is located at 59°44' N latitude and 137°44' W longitude in the extremely rugged and glaciated terrain of the Alsek-Tatshenshini River area of the St. Elias Mountains, in the northwestern corner of British Columbia (Fig. 1). The deposit crops out on Windy Peak at an elevation of 2,000 m. It was discovered by Frobisher Ltd., a subsidiary of Ventures Ltd., now Falconbridge Ltd., during follow-up of an aerial and regional reconnaissance geological survey of the St. Elias Mountains conducted in 1957 to explore for Triassic massive sulfides similar to the Kennecott deposit in Alaska. Sporadic exploration activity occurred from 1958 to 1980 and led to the conclusion that the property was too remote to be economic. In late 1983, Falconbridge conveyed title to the property to Geddes Resources, which conducted all subsequent exploration. Work between 1988 and 1991 included 4,139 m of underground development and 64,618 m of drilling in 55 surface and 147 underground diamond drill holes. Two large massive sulfide zones, termed the North sulfide body (NSB) and South

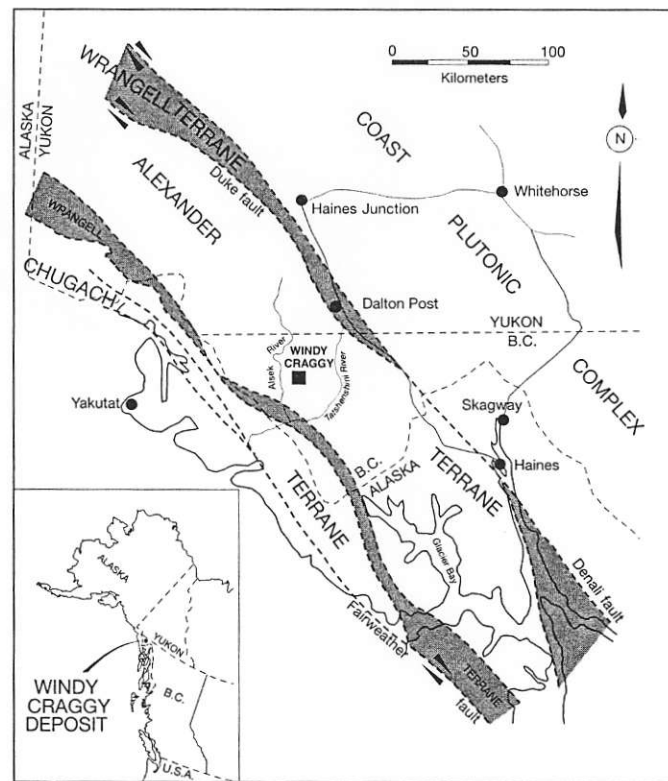


FIG. 1. Tectonic setting of the Windy Craggy area showing the distribution of Alexander, Wrangell, and Chugach terranes and the Coast Plutonic Complex (after Campbell and Dodds, 1983; MacIntyre, 1986); modified from Gammon and Chandler (1986). Inset: location of the Windy Craggy area in the extremity of northwestern British Columbia.

sulfide body (SSB), were outlined and likely a third zone (Ridge zone) was intersected by drilling. The latest (December 1991) total of proven, probable, and possible reserves is 297.4 million metric tonnes (Mt) grading 1.38 percent Cu at a cutoff grade of 0.5 percent Cu (Geddes Resources Ltd., 1991). The deposit is likely much larger than this as the limits of the NSB, SSB, and particularly the Ridge zone have not been delineated. The NSB alone (to December 1991) contains 138.3 Mt in all categories grading 1.44 percent Cu, 0.22 g/t Au, 4.0 g/t Ag, 0.066 percent Co, and 0.25 percent Zn. Other massive sulfide prospects,

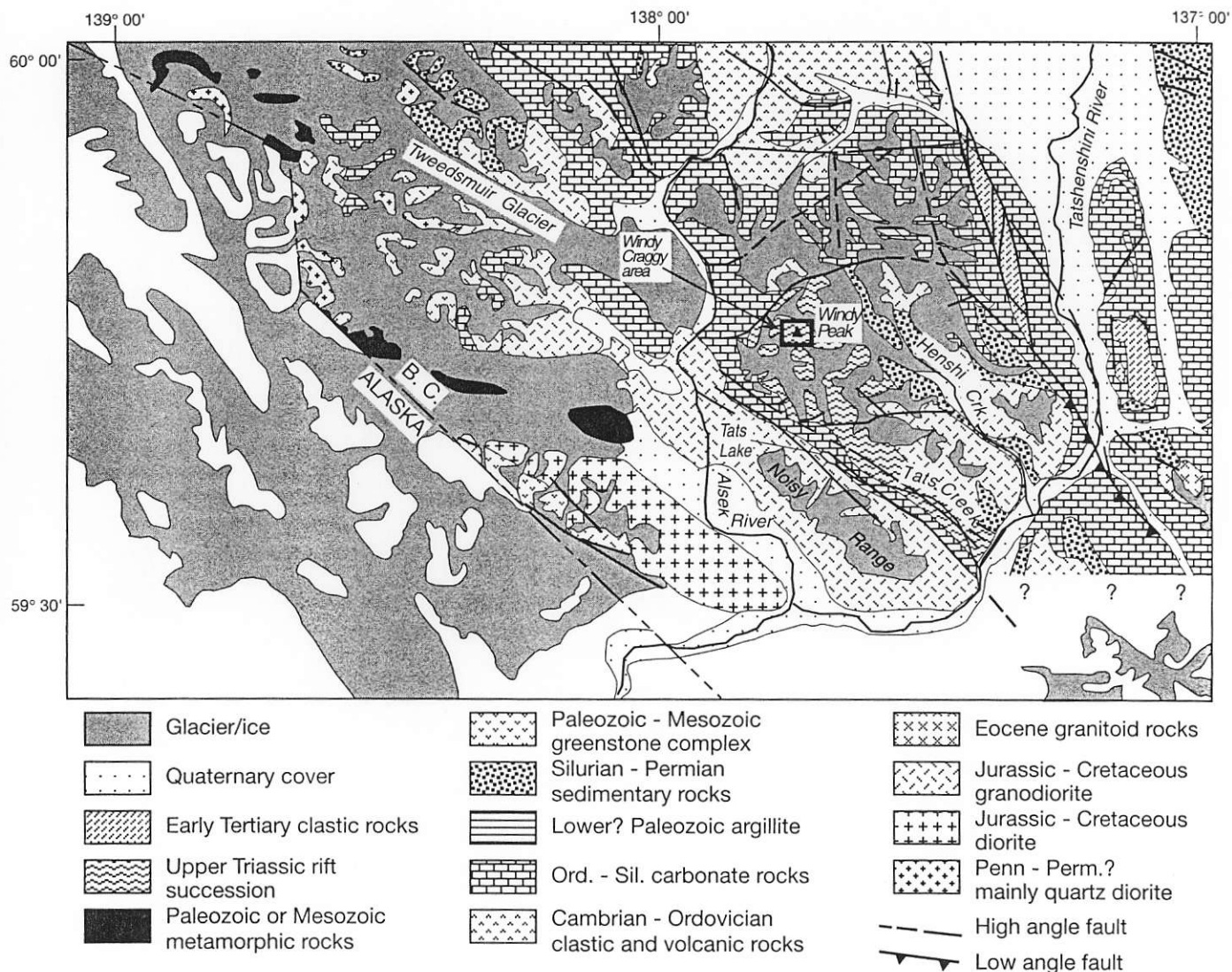


FIG. 3. Regional geology of the Tatshenshini River area (adapted from Mihalynuk et al., 1993). Box outlines area shown in Fig. 5.

sills (Fig. 4a). The lower volcanic division (LVD) is about 1,000 m thick, and consists of massive sills and basalt flows with minor interbeds of hornfelsed sedimentary rocks similar to those in the LSU (Fig. 4a). Dark green to black flows and sills are locally porphyritic with a microdioritic, felted texture. This unit is transitional between the LSU and the middle volcanic division (see below), and is not present in all localities. The middle volcanic division (MVD) is divided into a lower volcanic and sill-dominated section and an upper sediment-dominated sequence that hosts the Windy Craggy deposit (Fig. 4a). The MVD ranges from 600 to ~2,200 m in thickness, and consists of interbedded pillow basalt and graphitic to calcareous siltstone and argillite with minor tuff, chert, and limestone-clast debris flows. Basaltic sills are present locally, particularly in the upper sediment-dominated sequence. The graphitic and calcareous argillite beds are interpreted to be distal turbidites. Conodonts from graphitic and calcareous interbeds and from underlying graphitic and calcareous shales show

that the age of the volcanic and sedimentary rocks in the Windy Craggy area is Early Norian (225 Ma; Orchard, 1986). The upper volcanic division (UVD) ranges from 500 to 1,000 m thick and consists predominantly of massive to pillowed basalt flows with lesser basaltic sills; sedimentary rocks are rare to absent. A 50-m-thick agglomerate unit is present locally near the base of this unit (Fig. 4a).

The Upper Triassic section is in fault contact with a thick (>1,000 m) succession of lower Paleozoic (Ordovician to Silurian) gray limestones and silty limestones with intervals of thinly bedded, black- and rust-colored argillites (Fig. 3; e.g., Norford and Mihalynuk, 1994). The fine-grained clastics are thought to be coeval basinal facies equivalents of part of the platformal carbonate rocks. The carbonates are interpreted to have been deposited in a relatively shallow, subtidal marine environment; the paucity of evidence for widespread bioturbation or skeletal debris may indicate a hypersaline (Mihalynuk et al., 1993) and/or anoxic environment.

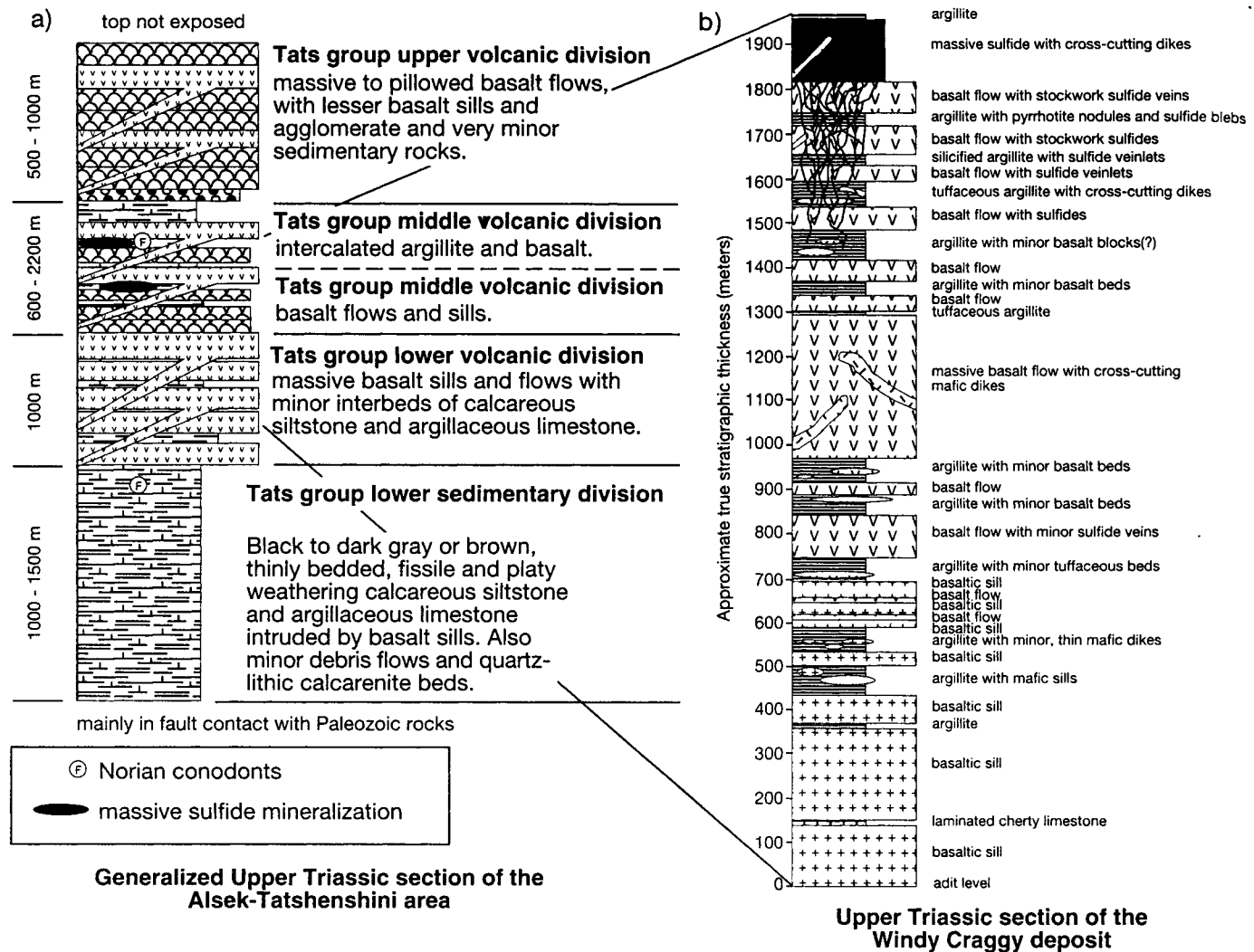


FIG. 4. a. Generalized Upper Triassic stratigraphic section for the Alesk-Tatshenshini area (from Mihalyuk et al., 1993); b. Detailed stratigraphic section of the Windy Craggy deposit. Compiled from underground geological mapping (Peter, unpub. data, and Geddes Resources Ltd.), drill core information, and surface mapping (J.M. Peter, unpub. data; MacIntyre, 1984; K. Dawson, unpub. data).

All rock types, including sulfide mineralization, are cut by mafic dikes that postdate the major penetrative foliation of the rocks they intrude (Peter and Scott, 1990). The deformational history and structural styles present in the Tatshenshini area are complex and highly variable. The main phase of ductile deformation, evidenced by tight to isoclinal folds and low-grade greenschist facies metamorphism, postdates deposition of the Tats group. Emplacement of Jurassic-Cretaceous plutons caused additional folding. Following this, the last phase of deformation resulted in the local development of penetrative shear fabrics and a crenulation cleavage, and in discrete faults and shear zones including large northwest-trending faults.

Deposit Geology

The upper sedimentary sequence of the Upper Triassic MVD is host to the Windy Craggy deposit (Fig. 4a, b). Surface mapping (Fig. 5) indicates the presence of massive to

pillowed basalt flows and sills, and calcareous argillite. Massive sulfide crops out on the very steep slopes of Windy Peak. Figure 4b is a stratigraphic section of the Windy Craggy host rocks and deposit, constructed from underground geologic mapping and drill core logs. Mafic igneous sills predominate in the southwestern map area (Fig. 5), in the lower part of the stratigraphic section, and are distinguished from dikes by field relations and trace element geochemistry (Peter and Scott, 1990; Peter, 1992). Massive to pillowed basalt flows predominate in the north and eastern parts of the area (Fig. 5) and constitute the middle to upper parts of the stratigraphic section (MVD). Although host rocks have been metamorphosed to greenschist facies, primary textures and structures typically are well preserved. Rocks are pervasively altered to chlorite, carbonate, albite, epidote, actinolite, sphene, and leucoxene.

Interpretation of the structural history of the Windy Craggy deposit and immediate environs is limited due to poor access to outcrops owing to the steep terrain and

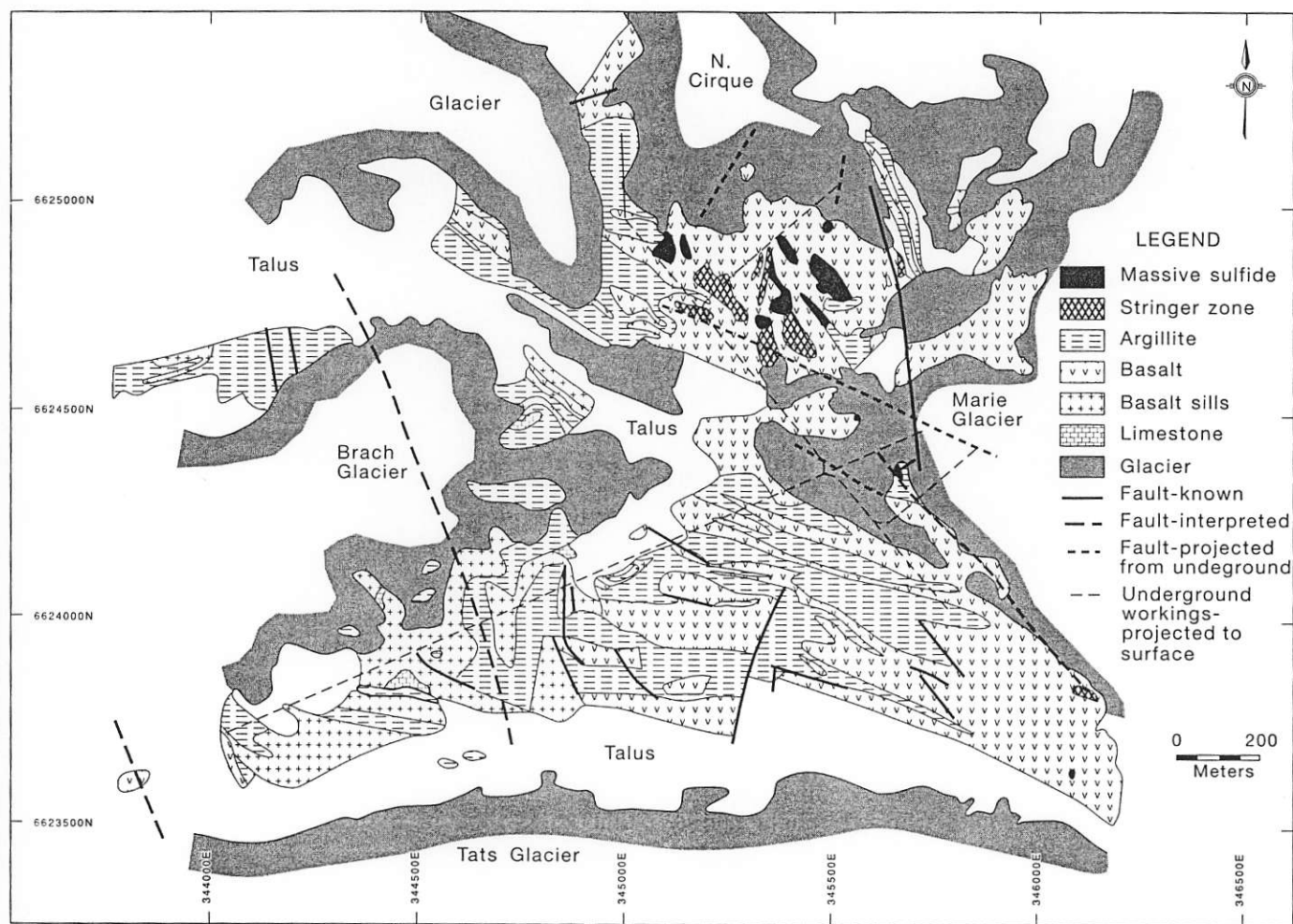


FIG. 5. Surface geologic map of Windy Peak (after Geddes Resources Ltd., unpublished map, 1991). Grid is in meters.

snow and talus cover, and lack of marker horizons. Mapping of the north face of Windy Peak by Kelemen and Radford (1983) identified two phases of folding. F_1 isoclinal folds trend northwest and west-northwest, and are deformed by F_2 open folds that trend north to northeast. F_1 folds commonly are overturned to the southwest and plunge 30° to 50° to the northwest. The plunge of the F_1 axes varies due to the influence of the steeply plunging F_2 folds. The thickness of the sulfides reflects isoclinal F_1 folding. Major faults dip steeply, strike northwest and trend subparallel to contacts between enclosing rocks (e.g., Fig. 5). Faulting is most prevalent within volcanic flows, diabase bodies, and sills. Narrow zones of shearing and faulting that contain slickensided chlorite and clay gouge are common in the diabase, and minor drag folds occur along shear and fault planes. High-angle normal and low-angle faults cut all older structures. Bedding and rock units trend northwest, and stratigraphic indicators such as normal graded beds and pillow forms indicate a sequence that youngs to the northeast. This is consistent with mineral zonation within the NSB and the position of its stringer zone to the south-southwest (see below).

Basalt Flows

Basalt flows, which predominate in the upper part of the stratigraphic section (Fig. 4), are massive to pillowed. Individual flows are up to 100 m thick and average 10 to 15 m. Scalloped contacts indicate that, in places, flows were deposited on unconsolidated, wet sediments. Flows are pervasively chloritized and carbonatized, and locally contain minor disseminated, fine-grained pyrite. Much of this alteration is related to a regional, lower greenschist facies metamorphic event (Forbes, 1986), and some to the hydrothermal system that produced the massive sulfides. The flows are generally only slightly foliated. They are fine-grained, range from medium gray to dark green, and commonly are vesicular to amygdaloidal, with amygdules 1 to 5 mm in diameter composed of white, fine-grained calcite and, rarely, fine-grained pyrrhotite. In places, amygdules comprise up to 4 vol percent of the rock. Less commonly, the flows are porphyritic, containing a randomly oriented network of euhedral plagioclase phenocrysts 3 to 8 mm in diameter and/or hornblende 0.5 to 3.0 mm in diameter with interstitial, very fine grained, felted chlorite

and fine-grained, disseminated sphene. The plagioclase laths locally are glomeroporphyritic, and variably altered to sericite, epidote, and calcite. Plagioclase is predominantly andesine (An₂₀ to An₄₀), consistent with the low calcium bulk chemical compositions. The values are atypical of unmetamorphosed basaltic rocks and probably have been modified during regional metamorphism. The hornblende phenocrysts are variably pseudomorphs of chlorite. Some of the porphyritic basalts have euhedral plagioclase that is altered to albite containing abundant inclusions of actinolite and epidote.

Relict clinopyroxene and orthopyroxene are present locally, although they commonly are altered to chlorite, biotite, actinolite, epidote, and quartz. Colorless to pale brown clinopyroxene (augite) is present as subhedral grains 0.2 to 1 mm in diameter in the groundmass of some samples. It ranges from nearly fresh grains with only narrow pale green actinolite reaction rims to small anhedral remnants in the centers of chlorite-actinolite pseudomorphs.

Groundmass plagioclase, like the phenocrysts, is altered to white mica and albite. The opaque phases are mostly titanomagnetite, which displays sphene-like alteration rims, and small disseminated pyrite crystals. Blue-green actinolite and pale green chlorite are also present as randomly oriented needles and patches in the groundmass. These minerals lack obvious relation to primary minerals and may be replacing former glass. In addition, anhedral grains of epidote and calcite are abundant in the groundmass of some samples. The amygdules are filled primarily with chlorite, calcite, and quartz, with minor actinolite and epidote. All of the above secondary minerals are characteristic of greenschist facies metamorphism.

Basaltic Sills and Dikes

Sills vary in thickness from 1 to 40 m and are medium-grained, and medium to dark green. They are composed predominantly of plagioclase and hornblende phenocrysts, typically up to several millimeters in diameter, in a finer grained chloritic matrix. Accessory minerals include leucoxene and sphene.

Medium- to coarse-grained diabasic dikes were intersected in drill core. They are composed of interlocking crystals of plagioclase, amphibole and pyroxene, and, in part, display an ophitic texture (Harris, 1988). Locally, the dikes have biotite pseudomorphs after hornblende phenocrysts. They are moderately to intensely altered to chlorite, calcite, and epidote. These rocks locally host stockwork or stringer mineralization and therefore predate mineralization. The diabase bodies are geochemically similar to footwall and hanging-wall flows (see below), and are cogenetic with them and are likely the feeder conduits for these overlying volcanic units.

Cumulate rocks are rare and have only been noted in drill core; they occur at the base of gabbro bodies. It is not known if they are concordant or discordant. These rocks consist of randomly intergrown, ragged clinopyroxene, orthopyroxene, pale amphibole (tremolite), brown amphibole, and olivine. Minor amounts of partly chloritized dark brown biotite, traces of euhedral apatite, and fine-grained

disseminated rutile are also present. These rocks invariably are intensely altered.

Late Dikes

Unmineralized late mafic dikes, ranging from 10 cm to several meters in width, are generally lighter in color (pale gray-green) and finer grained than sills. They typically have a 1- to 20-cm-wide chloritic chilled margin. Some have homogeneous, ophitic meshwork textures, whereas others are porphyritic. Plagioclase and amphibole are the dominant minerals with sericite and plagioclase alteration and local biotite pseudomorphs after hornblende phenocrysts. These dikes crosscut all rock types, including massive sulfides. In some places, the dikes also crosscut the regional penetrative foliation, but in others the dikes themselves are slightly to moderately foliated. On this basis, dike emplacement is interpreted to postdate peak metamorphism and deformation. Mihalyuk et al. (1993) noted the presence of dioritic to gabbroic intrusive rocks which range from Cambro-Ordovician to Tertiary age in the area, and the late dikes at Windy Craggy may be related to these rocks.

Argillite

Most of the sedimentary rocks in the immediate vicinity of the deposit are fine- to very fine grained, gray-, black-, brown-, or silver-weathering, indistinctly to well-laminated argillite, with rare limy, sandy, and sedimentary breccia beds. Individual argillite units range from several centimeters to about 40 m thick, but on average are 10 to 15 m thick. The argillites may be calcareous, non-calcareous, and/or carbonaceous. They are indistinctly to well laminated (<1 mm to 20 cm). Thin, sandy lenses or beds containing pale gray calcareous grains are an extremely minor component.

Argillite is composed of quartz, carbonate (calcite), chert, and carbonaceous material that occurs as sub-micron-sized inclusions, with graphite as foliae, and with sericite, plagioclase, biotite, chlorite, pyrite, and pyrrhotite. The carbonate likely originates from the erosion of Devonian limestone to the west(?); supporting evidence comes from the presence of both Norian (Upper Triassic) and Devonian conodonts in a carbonate debris flow in the immediate hanging wall of the Windy Craggy deposit (MacIntyre 1983). The presence of abundant carbonate indicates that the sediments were not deposited at depths below the carbonate compensation depth. In places, the argillite contains a significant tuffaceous component that consists of dark green, chlorite-rich beds and laminae that are mainly resedimented turbidites. Some of the tuffaceous beds contain plagioclase laths in a chloritic matrix. In an idealized Bouma sequence (Bouma, 1962), all samples would be classified as distal turbidites (Bouma units E-mud, and possibly some D-interlaminated mud and silt). Minor pelagic sediments are also present, and include thin black graphitic horizons interbedded with volcanic flows and turbiditic argillites.

Sedimentary structures include normal graded layering, scours, pebble dets, and concretions composed of

pyrrhotite, pale gray calcite, ferroan dolomite, stilpnomelane, chlorite, actinolite, and rare blebs of chalcopyrite. Soft-sediment deformation, represented by slump structures, indicates that the basin was tectonically active during sedimentation. Macrofossils are very rare, and only one dense accumulation, several meters wide, of Triassic *Rynchonellid* brachiopods (genus *Halorela*; Ager, 1965; p. 605; J. Waddington, pers. commun., 1991) 1 to 2 cm in diameter was found in the immediate vicinity of the deposit, well down in the footwall sill-argillite sequence.

Argillite contains minor, very fine to coarse-grained, disseminated euhedral cubes of pyrite and/or fine-grained pyrrhotite, of either syngenetic or diagenetic origin. Sulfide-rich beds and laminae occur in a few places, commonly with diagnostic framboidal pyrite textures. Sulfide-rich argillite grades locally into semi-massive sulfide. Epigenetic sulfides (pyrite, pyrrhotite, and chalcopyrite) locally occur as discrete layers that have selectively replaced beds;

copper grades of this material are generally <0.5 wt per cent. Some argillite displays a well-developed foliation defined by pyrrhotite plates that are aligned in an axial planar orientation. A slaty cleavage is variably developed within graphitic argillite.

Mineralization

Drilling and underground development have identified two main sulfide zones, the North and South sulfide bodies (NSB and SSB, respectively), each with an underlying, variably developed stockwork/stringer zone; a third, apparently smaller, massive sulfide body and associated stringer mineralization is named the Ridge zone. Figure 6 is a 1,400-m level plan of the explored and developed parts of the Windy Craggy deposit showing the extent of mineralization and intercalated volcanic and sedimentary rocks. The tabular to lenticular NSB trends west-northwest and dips moderately steeply to the north-northeast. True

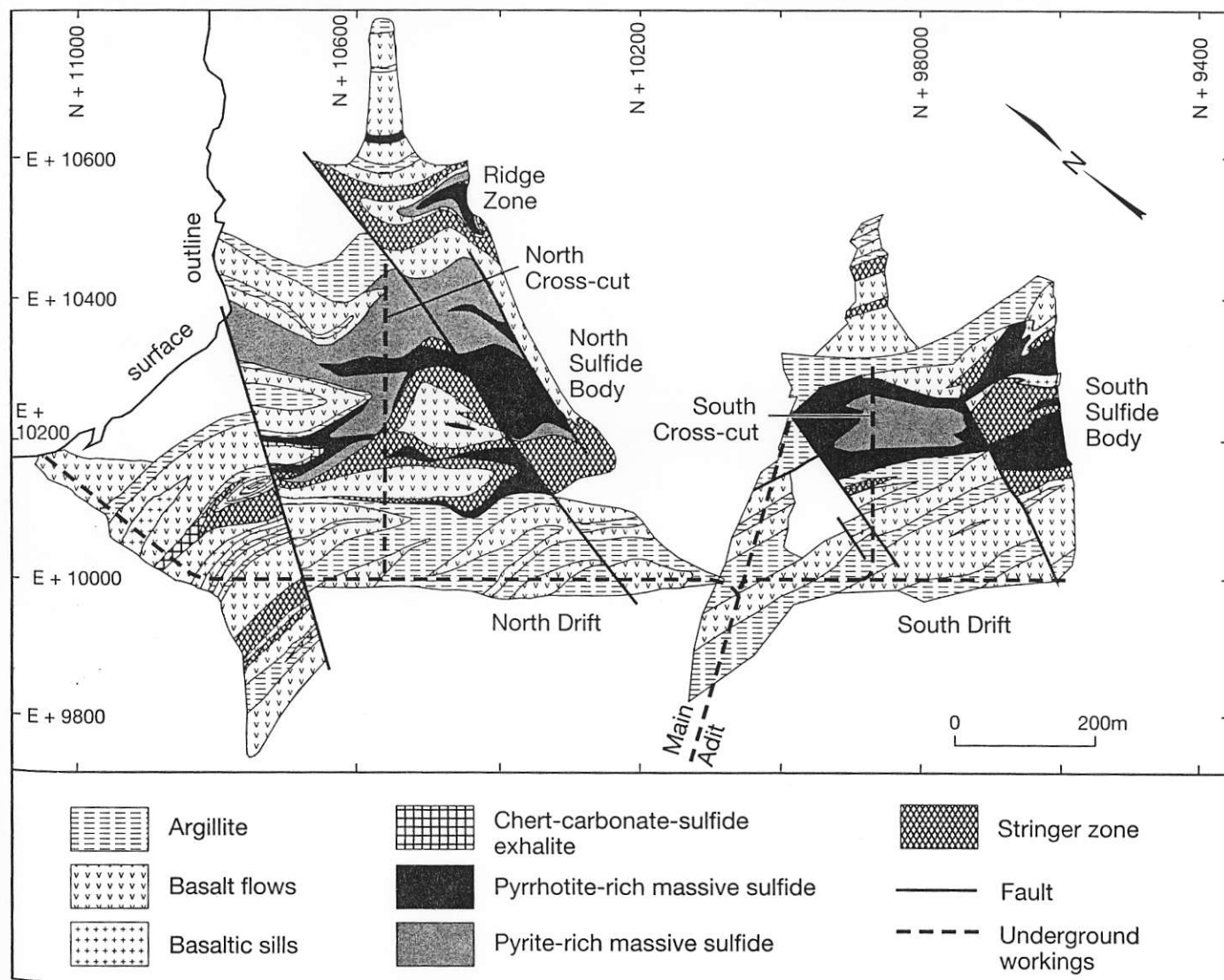


FIG. 6. 1,400-m level plan (exploration adit level) of the explored, drilled, and developed portions of the Windy Craggy deposit (after Geddes Resources Ltd., unpublished plan, 1990). White areas indicate no geologic data available; grid is in meters.

dimensions for the NSB are a thickness of about 120 to 150 m thick and a diameter of about 500 m (Fig. 7). The NSB is mineralogically zoned from a pyrrhotite-rich core that passes stratigraphically upward to pyrrhotite + pyrite, to overlying pyrite-rich massive sulfide and to massive pyrite + calcite + sphalerite (Fig. 7), to a discontinuous cap of exhalites (Fig. 6). Magnetite occurs at the transition from pyrrhotite to pyrite, as fine-grained wisps, blebs, and patches; this zonation is probably a primary feature.

The tabular to lensoid SSB plunges steeply to the southeast and extends to the southeast (Fig. 8). The strike of the SSB is generally discordant with the enclosing host rocks, suggesting that the present geometry is due to structural modification. The SSB (Fig. 8) is relatively more deformed, such that its primary morphology has been changed. Primary zonation in the SSB has largely been obliterated by folding and/or translation of the sulfide mass during deformation. The SSB now consists of a pyrrhotite-rich outer periphery and a pyrite-pyrrhotite-magnetite core containing about 50 percent pyrite with equal amounts of pyrrhotite and magnetite and only a few percent chalcopyrite.

At the 1,400-m level (the level of the adit), massive sulfide mineralization is about 200 m wide, extends for an almost continuous strike length of 1.6 km horizontally, and shows only about a 250 m separation between the NSB and SSB (Fig. 6). From surface, mineralization extends at least 600 m vertically (Figs. 7, 8), and both the NSB and SSB remain open at depth and along strike. Our interpretation is that the NSB and SSB likely formed as discrete lenses that originally were not contiguous, and these were subsequently faulted and displaced from each other. Evidence for this comes from the different geometries of the bodies

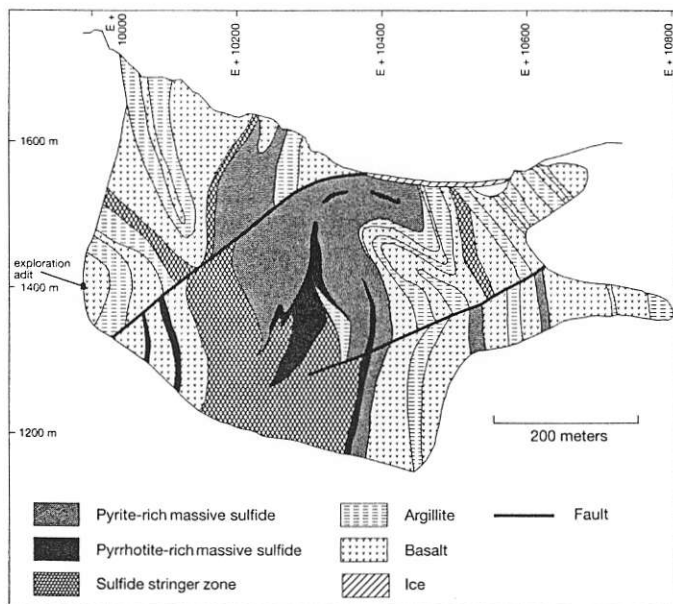


FIG. 7. Cross section of the North sulfide body (NSB) looking west; section 10570N (after Geddes Resources Ltd., unpublished cross section, 1990). White areas indicate no geologic data available; grid and elevation are in meters.

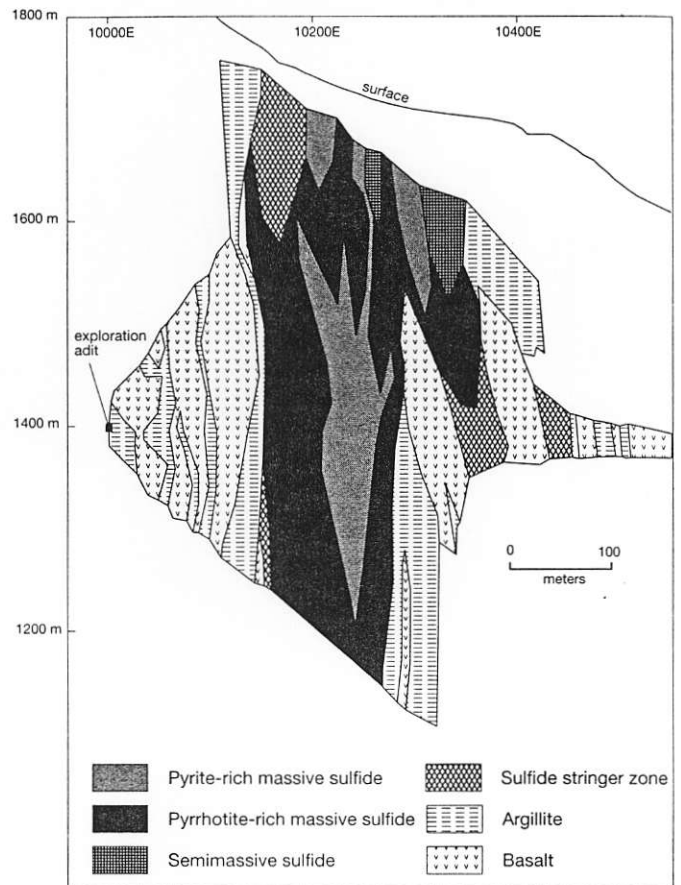


FIG. 8. Cross section of the South sulfide body (SSB) looking west; section 9850N (after Geddes Resources Ltd., 1990). White areas indicate no geologic data available; grid and elevation are in meters.

and their different Zn contents. The stratigraphic upper part of the NSB is relatively Zn-rich, grading 2.02 wt percent over 12 m and the lower 188 m grading 0.54 wt percent, whereas the SSB is essentially devoid of Zn. Although the Ridge zone is distinct from the main massive sulfide bodies (Fig. 6), there are insufficient data to interpret its structural relationship to the NSB and SSB, or to determine its mineral zonation. However, there is appreciably more sphalerite and chalcopyrite in the Ridge zone than in the bulk of the NSB and SSB.

A particularly gold-rich part of the deposit (gold values up to 14.7 g/t over 29.7 m; Northern Miner, 1983, 1988) occurs at the northwestern edge of the SSB near the end of the main adit (Fig. 6), at the intersection of two major faults within a gold-enriched chert-carbonate-sulfide chemical sediment or exhalite. Gold was likely mobilized from the exhalite into the fault zones by later hydrothermal fluids.

Massive Sulfide

In the NSB, textures that appear primary are best preserved in the stratigraphic upper parts of the lens (east end of the North crosscut), whereas they are largely obliterated in the pyrrhotite-rich core (west end of the North crosscut). With a few exceptions, primary textures are

largely absent in the intensely sheared and recrystallized SSB. Within the massive sulfide, mottled, fine-grained carbonate patches are locally abundant. Carbonate is predominantly white to black calcite, with minor amounts of pale brown siderite. Chalcopyrite as wisps, streaks, and blebs is associated with the carbonate.

Although most of the sulfides are fine- to very fine grained and relatively featureless, the following textures are present: (1) minor laminated to bedded sulfides consisting

of pyrrhotite, magnetite, pyrite, and chalcopyrite, with carbonaceous interbeds and laminae (Fig. 9a). Where sulfides are interlaminated with such material, the principal mineral is very fine grained pyrrhotite. This material has been noted to occur predominantly at about 10,125 m E in the south crosscut (Fig. 6). This primary texture, which is easily confused with relict argillite beds and laminae that have been partly to completely replaced by pyrrhotite and lesser chalcopyrite (Fig. 9b), is common where stockwork

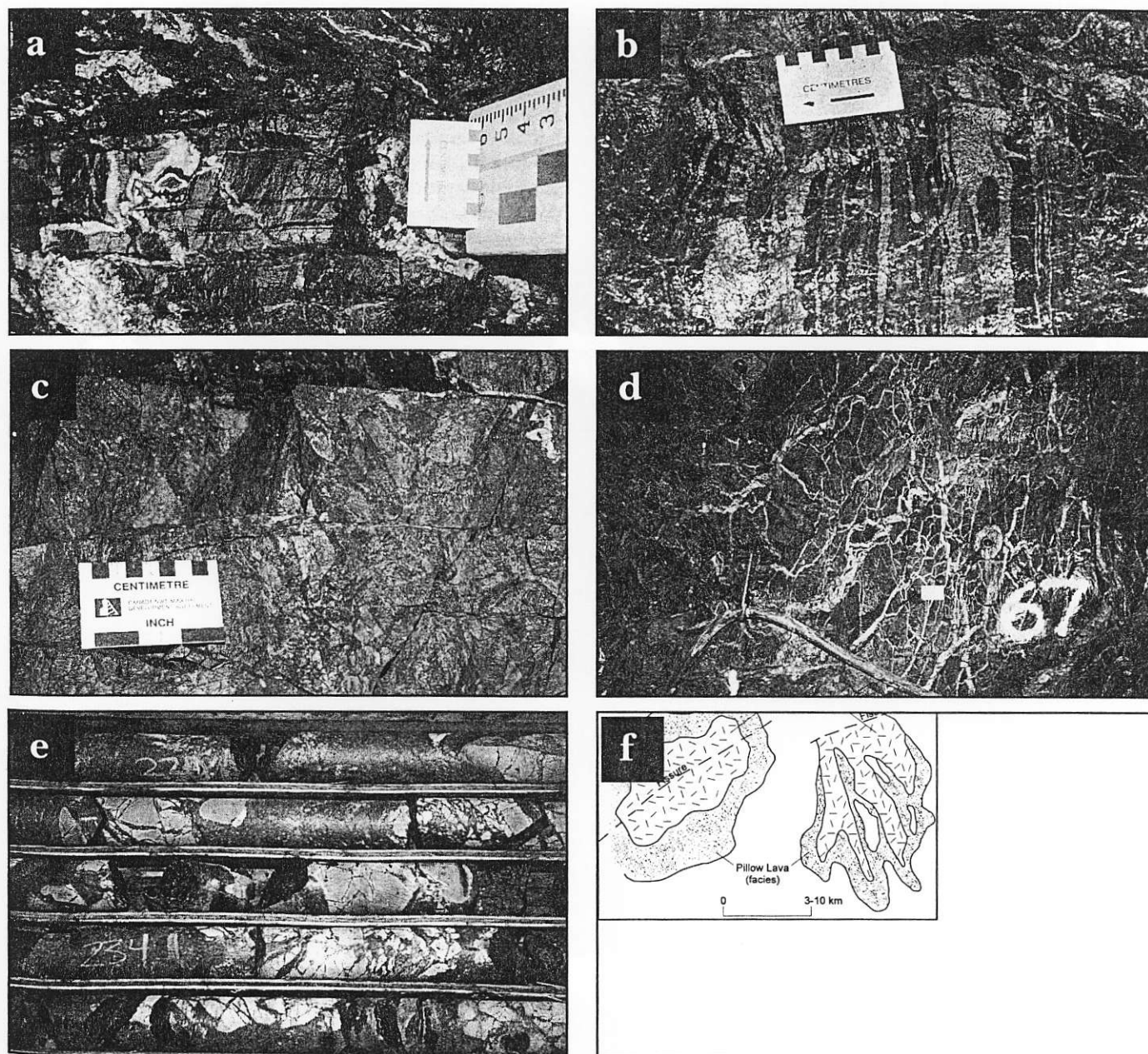


FIG. 9. a. finely laminated pyrrhotite-rich sulfide with minor argillaceous interbeds and crosscutting quartz-ankerite veinlets in immediate footwall, south crosscut at 125 m, north wall, SSB (South sulfide body). Arrow (on scale) indicates younging direction; b. argillite laminae that have been silicified and partly replaced by pyrrhotite and chalcopyrite, north crosscut, NSB (North sulfide body); c. sulfide breccia composed of pyritic sulfide clasts in a pyrrhotite-rich matrix, north crosscut at 110 m, south wall, NSB; d. stockwork pyrrhotite + pyrite + chalcopyrite vein network in chloritized basalt, north crosscut, NSB. Small white, rectangular scale card is 8.5 cm long; e. silicified, bleached, and brecciated basalt with veins and matrix composed of pyrrhotite + pyrite + chalcopyrite, drill core, NSB (core diameter = 3.5 cm); and f) sample of exhalite with chert, carbonate, and sulfide laminae, north crosscut, NSB.

veins cut laminated to bedded argillite; (2) colloform layered calcite, siderite, and pyrite within fine-grained massive sulfide; this texture is suggestive of open-space filling and implies that cavities and fractures were present in the sulfide mass; (3) brecciated massive sulfides consisting of angular pyrite-rich clasts in a finer grained pyrrhotite-rich matrix (Fig. 9c) that are common in the NSB; these matrix-supported clasts range from 1 to 30 cm in diameter and typically comprise a few to tens of per cent of the total volume of mineralization. The brecciated or clastic texture is interpreted to have been the product of recementation of talus eroded from collapsed sulfide chimneys and mounds. Locally, the clasts are slightly to intensely deformed and stretched. Particularly in the North crosscut (Fig. 9c), relatively undeformed, angular and brecciated sulfides can be traced into foliated sulfides that display fine banding and indicate that the banding is due to extremely deformed sulfide clasts; (4) recrystallized, spongy, medium- to coarse-grained pyrite. The absence of this texture in the SSB and its presence in the NSB indicates that it is probably primary and unrelated to metamorphism and deformation. Alternatively, it could reflect greater deformation of the SSB; (5) foliated sulfides with alternating, essentially monomineralic, discontinuous wisps, lenses, and bands of chalcopyrite, pyrite, pyrrhotite, calcite, and magnetite. Generally, foliated sulfides are much more prevalent in the SSB and probably formed by folding and recrystallization during deformation.

Stockwork or Feeder Zone

A discordant stockwork sulfide zone is present beneath the NSB, SSB, and Ridge zone (Figs. 5, 7, 8), although it is better developed, or its primary morphology is better preserved, in the less deformed NSB. Deformation of the stockwork zones at Windy Craggy accounts for their lack of a pipe-like morphology common to many massive sulfide deposits. However, in the NSB, sulfide veins cut volcanic stratigraphy. Stockwork mineralization occurs within foot-wall basalt, intrusive rocks, and argillite. It consists of irregular veinlets of sulfides less than 1 mm to about 1 m wide within pervasively chloritized and/or silicified and brecciated host rocks (Fig. 9d, e), and as small lenses or pods of sulfide up to several meters in diameter. Fine-grained disseminated sulfides also occur within the host rocks.

The NSB has a well-developed stockwork/alteration zone within both volcanic and sedimentary rocks that extends at least 200 m stratigraphically beneath the base of massive sulfides. Sulfides within the stockwork zone consist predominantly of pyrrhotite with lesser chalcopyrite and, in places, pyrite and sphalerite. Within the relatively undeformed stockwork zone, chalcopyrite occurs as fracture fillings in pyrite. The percentage of sulfides, and the number and density of sulfide veins, increase upward from the bottom or "root" to the top of the stockwork zone. Copper contents within the stockwork range up to 1.5 wt percent; in the NSB, a 58 m section grades 1.07 wt percent Cu. Gangue minerals include quartz, carbonate, chlorite, and albite.

The NSB stockwork displays distinct zoning of alteration minerals. The most intensely altered zones are characterized

by moderate to extreme bleaching and silicification of host basalt rocks (Fig. 9e). Accompanying this silicification is slight to intense brecciation of the host basalts and veins of pyrite, pyrrhotite, chalcopyrite and, locally, minor quartz and/or sphalerite. Host basalt breccia fragments have been weakly to intensely chloritized and/or bleached and silicified. Fragments are angular, 1 to 10 cm in diameter, translucent, and milky white. Intensely altered rocks resemble cryptocrystalline chert. In places, sulfides infill pillow interstices and radial shrinkage or cooling cracks within pillows. The narrowest and most closely spaced sulfide veinlets are associated with the most intense silicification, giving the appearance of a crackle breccia. These strongly silicified zones presumably represent the most intense fossil hydrothermal up-flow zones. Silicification grades laterally into pervasive chloritization, although there is no consistent relationship or zonation observed between the occurrence of silicified basalts, chloritized basalts, and massive sulfides. The most intense chloritization typically occurs adjacent to the zone of silicification and is characteristically a distinctive, bright, apple-green. This variety of chlorite grades laterally away from the stockwork zone to a darker olive-green chlorite. Compositional differences between these types of chlorite are discussed below.

Stockwork mineralization in argillite consists of pale to dark gray argillite fragments in a fine-grained sulfide matrix; such mineralization in tuff generally contains darker gray-green fragments. These tuff fragments commonly are more chloritic, reflecting their basaltic precursor mineralogy. Intensely altered argillite and tuff fragments are cryptocrystalline and milky white. Relict layering is present in both argillite and tuff. Pyrrhotite and chalcopyrite occur along selected laminae and beds within individual fragments as replacements of coarser-grained laminae and beds, and veinlets of these sulfides interconnect these sulfide layers. Sulfides also occur as infillings of open space between breccia fragments. Quartz precipitated in zones of intense silicification where it pseudomorphs igneous minerals.

Supergene Mineralization

An oxidized limonitic cap up to 90 m thick overlies outcropping massive sulfide (not shown in Figs. 7 and 8). Supergene minerals include limonite, chalcocite, native copper, chalcantite (copper sulphate), melanterite, malachite, azurite, and possibly cuprite, hematite, sphalerite, recrystallized pyrite, silica, and minor magnetite. This supergene mineralization grades to over 12 wt percent Cu in places. Approximately 2 Mt of such material has been delineated, the majority of which occurs under Marie Glacier (Fig. 5).

Hydrothermal Sediment

Hydrothermal sediment or "exhalite" is finely laminated to bedded (<1 mm–5 cm) chert-carbonate-sulfide (Fig. 9f); individual exhalites are generally too thin (0.1–3 m) to be shown as mappable units on Figures 4, 7, and 8. The exhalite has a reddish to pale-greenish gray color imparted by abundant iron oxides (hematite) and chlorite.

Other contained minerals are calcite, siderite, ankerite, chert, sericite, rutile, magnetite, pyrrhotite, pyrite (typically framboidal or colloform), chalcopyrite, and, rarely, sphalerite, arsenopyrite, gold, and electrum. At the SSB, hydrothermal sediment occurs immediately below the structural and stratigraphic base. At the western margin of the NSB several thin exhalite units are intercalated with basalt flows that immediately overlie massive sulfides in the stratigraphic hanging wall (Fig. 6). The areal extent of the exhalite at Windy Craggy is not well defined because of limited exposures. Surface mapping indicates that the exhalites are not laterally extensive and they likely cover an area several times that of the massive sulfide bodies themselves, similar to the *tetsusekiei* in the Japanese Kuroko deposits (e.g., Kalogeropoulos and Scott, 1983).

The fine-grained, laminated nature of the exhalite and its alternating monomineralic layers of pyrite, pyrrhotite, carbonate, quartz, chlorite, and magnetite in many places, and the framboidal and colloform nature of the pyrite, are all indicative of a hydrothermal sedimentary origin. Chalcopyrite is present as fracture fillings, fine-grained disseminations, and banded grain aggregates. Rare gold and electrum are 7 to 8 μm in diameter. Siderite occurs in several forms: (1) very fine grained, structureless, micritic aggregates 2 to 10 μm in diameter; (2) subhedral to rhombic grains 0.05 to 0.2 mm in diameter; (3) tan to brown, very fine grained, colloform-layered spheres and atoll structures that locally have coalesced to produce a delicate laminar texture. Chert is extremely fine grained, ranging from <5 to 15 μm diameter and contains finely disseminated minute shreds of chlorite. Fine-grained microlites of plagioclase are locally present. The chlorite, sericite, and plagioclase probably reflect a tuffaceous or detrital sedimentary component as these aluminosilicates are not ordinarily precipitated from submarine hydrothermal solutions on the sea floor.

In places, the exhalites are brecciated and contain angular clasts of fine-grained, hematitic quartz in a hematitic quartz \pm sulfide (pyrite, pyrrhotite, chalcopyrite, sphalerite) matrix. Hematite and chert-rich exhalite fragments commonly display millimeter- to centimeter-wide, very fine grained, bleached rims. Sulfidized exhalite is present in the lower part of the NSB and at the base of the SSB, and is characterized by sulfide veinlets and pseudomorphs after hematite. The presence of exhalite that has been partly replaced by sulfide indicates that such rocks may have been formed and destroyed more than once during sulfide formation at Windy Craggy. The occurrence of "early" exhalite in both the NSB and SSB indicates that chemical sedimentation occurred in the area in the early stages of sulfide deposition.

Mineralogy and Mineral Associations

Opaque minerals within the massive and stockwork bodies include pyrite, pyrrhotite, chalcopyrite, sphalerite, marcasite, galena, digenite, arsenopyrite, an unidentified bismuth telluride, cobaltite, cubanite, native gold, electrum, and native silver. Gangue minerals are: siderite, calcite, ankerite, magnetite, quartz, chlorite, stilpnomelane, and

hisingerite, with trace barite. Primary textures are better preserved in the NSB than in the SSB due to the less intense deformation of the former.

Pyrite ranges from less than 5 μm to several millimeters in diameter. In the NSB two generations are recognized: (1) early, colloform to framboidal spheres and colloform layers (Fig. 10a). This pyrite contains inclusions of gangue minerals and other sulfides that appear to define growth surfaces. Individual colloform pyrite layers are distinguished by fine-grained inclusions of non-sulfide gangue. Some pyrite framboids and colloform layers are partly replaced by pyrrhotite and chalcopyrite; (2) later, recrystallized, euhedral cubes and pyritohedra intergrown in a boxwork fashion; some is incipiently fractured and veined by chalcopyrite and pyrrhotite (Fig. 10b, c). This variety of pyrite locally overgrows the colloform variety with little or no replacement. Euhedral pyrite grains commonly contain numerous inclusions of gangue minerals, pyrrhotite, and chalcopyrite. Locally, these inclusions are concentrated along growth zones and were probably incorporated during recrystallization of the pyrite. In the SSB, pyrite is present as the latter variety only, typically forming trails of cataclastic and comminuted grains.

Pyrrhotite (50 μm to 0.5 mm) is interstitial to pyrite, fills fractures in pyrite together with chalcopyrite, and also forms small inclusions within pyrite. In the SSB, pyrrhotite grains are elongate and display rare deformational twin lamellae. In places in both the NSB and SSB, pyrrhotite is completely recrystallized to a crystalloblastic/granoblastic texture with 120° grain boundaries or to elongate, deformed, foliated grains. In highly deformed samples, deformation twin lamellae are developed. Staining with a magnetic colloid indicates the presence of magnetic domains in primary, single phase ferrimagnetic monoclinic pyrrhotite (Kissin, 1974) (Fig. 10d).

Chalcopyrite displays mutual boundaries with pyrrhotite and occurs as blebs interstitial to pyrite and as fracture fillings in pyrite, together with pyrrhotite (Fig. 10c). A small amount of chalcopyrite forms minute (<10 μm) inclusions within pyrite. In places, early pyrite spheres are partly pseudomorphed by chalcopyrite, and in the more highly deformed SSB, some chalcopyrite shows deformation twin lamellae.

Sphalerite grains 5 to 500 μm in diameter are interstitial to euhedral pyrite and display mutual boundaries with pyrrhotite. The mineral is not compositionally zoned. Sphalerite is rarely present in the SSB, occurring as small, isolated, anhedral grains within carbonate and as narrow veinlets cutting other sulfides. Marcasite is prevalent only within the SSB, where it forms minute, rounded blebs and euhedral, hexagonal inclusions in pyrrhotite. Galena has been noted by previous workers (e.g., Gasparrini, 1983; McCarthy and Robinson, 1991) as overgrowths on pyrite, as small inclusions in pyrite and pyrrhotite, as small grains intergrown with chalcopyrite and/or sphalerite, and with chalcopyrite and sphalerite fracture fillings in pyrite.

Digenite has only been observed in the NSB. It forms inclusions within chalcopyrite and also occurs as irregular, anhedral blebs with chalcopyrite and sphalerite, with which it displays mutual boundaries interstitial to, and as

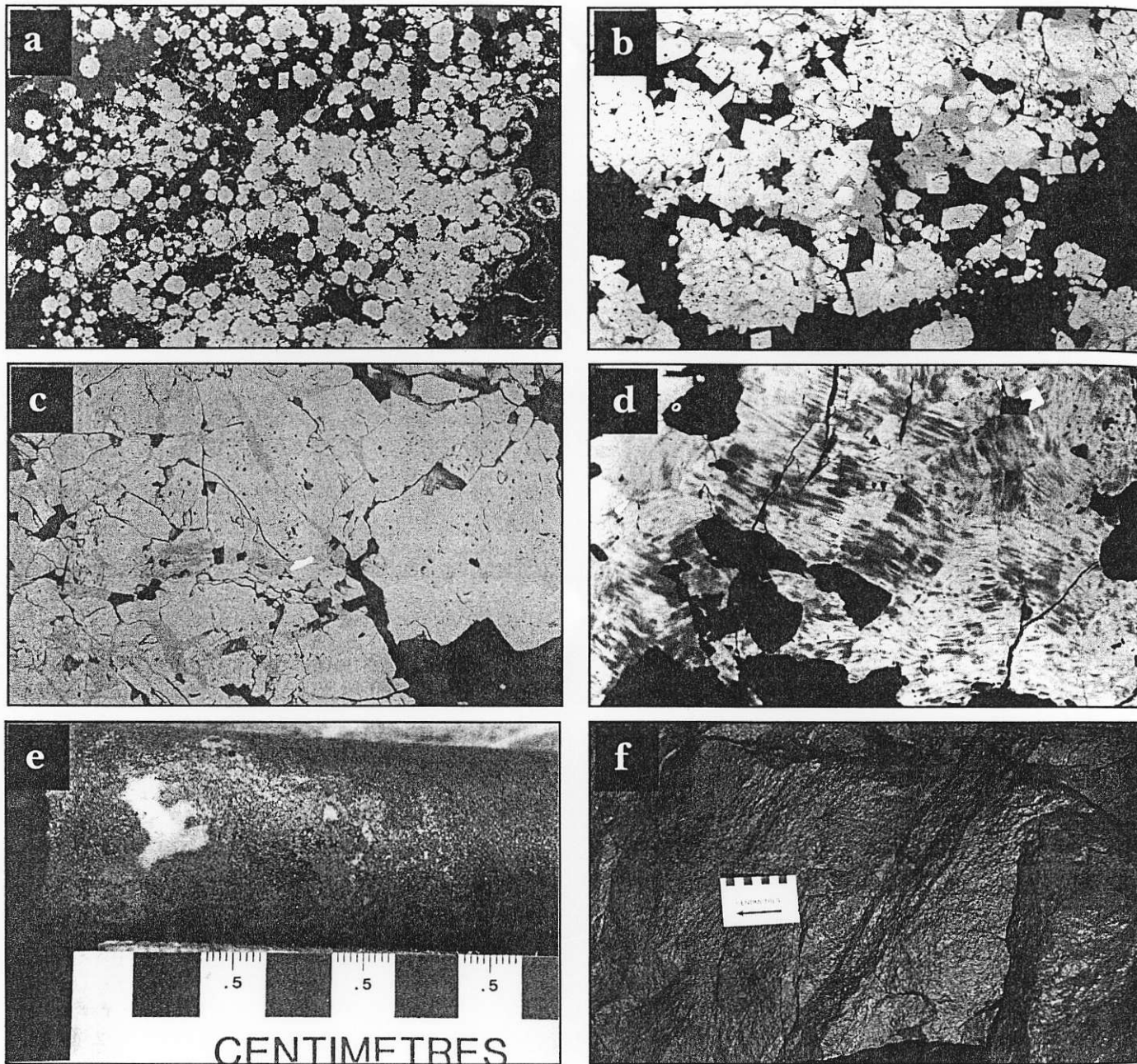


FIG. 10. a. reflected light photomicrograph showing framboidal pyrite spheres with colloform pyrite overgrowths in matrix of quartz, field of view (FOV) = 3.4 mm; b. reflected light photomicrograph showing recrystallized pyrite cubes with interstitial chalcopyrite and chalcopyrite (medium gray) filling fractures, with matrix of quartz (black), FOV = 1.2 mm, sample 88-41; 303.8 m, SSB; c. reflected light photomicrograph showing angular, 12 μ electrum grain (white) and chalcopyrite (medium gray) filling fracture in pyrite, FOV = 0.19 mm, sample 88-43; 189.6 m, SSB; d. reflected light photomicrograph of pyrrhotite stained with magnetic colloid showing the presence of magnetic domains (medium to dark gray) in primary, single-phase, ferrimagnetic monoclinic pyrrhotite (light gray) in quartz and calcite gangue (black), FOV = 0.50 mm; e. calcite patch (white) with outer rim of siderite (gray) in massive pyrrhotite, drill core, NSB; f. bifurcating magnetite vein (black) within massive sulfide, south crosscut, SSB.

overgrowths on, pyrite. Rare arsenopyrite within massive sulfides forms subhedral grains intergrown with framboidal and euhedral pyrite, chalcopyrite, sphalerite, and pyrrhotite. Arsenopyrite is also present in trace amounts within exhalite units associated with both the NSB and SSB, where it forms 10- to 30- μ m-diameter euhedral rhombohedra or lozenge-shaped crystals that have chalcopyrite and

pyrrhotite overgrowths. Bismuth telluride forms very small rounded blebs in pyrrhotite. Its presence was identified by scanning electron microscopy, and optical properties suggest one of the following minerals: wehrlite (BiTe), hedleyite ($\text{Bi}_{14}\text{Te}_6$), or tellurobismuthinite (Bi_2Te_3). Cobaltite occurs as discrete grains within a narrow carbonate veinlet (Mainwaring, 1983), and as small, euhedral cubes within

pyrrhotite (Buchan, 1983). Cubanite and valleriite have also been noted (McCarthy and Robinson, 1991).

Native gold and electrum occur in both the NSB and SSB as (1) blebs filling fractures in pyrite together with chalcopyrite and pyrrhotite, in massive sulfide (Fig. 10c); (2) anhedral inclusions within recrystallized, euhedral pyrite in massive sulfide; and (3) inclusions within, and intergrowths with, calcite in gold-enriched portions of the chert-carbonate-sulfide exhalite unit. Limited electron microprobe analyses indicate that the gold is over 95 percent pure with minor silver and trace copper (McCarthy and Robinson, 1991). Native silver was identified by Buchan (1983) in massive sulfide as (1) inclusions in pyrite, (2) fracture fillings in pyrite, (3) discrete grains displaying mutual boundaries with pyrite, and (4) inclusions in pyrrhotite.

Siderite occurs within massive sulfide as early, inclusion-bearing, brownish, anhedral crystals and patches that form colloform to botryoidal overgrowths on sulfides. Euhedral brownish siderite rhombs generally display growth zoning. Siderite is commonly overgrown by calcite that occurs as interstitial, anhedral, optically clear, white or dark gray to black anhedral grains. Calcite typically forms discrete patches (Fig. 10e) or intergrowths of black and white varieties. Minor euhedral rhombs of ankerite are present in microcrystalline quartz as well as in granular zones within siderite and sulfides.

In the NSB, magnetite is a relatively minor component, occurring as euhedral dodecahedra and octahedra that occur within pyrite, pyrrhotite, chalcopyrite, carbonate, and rarely, sphalerite. In the SSB, magnetite is abundant as bifurcating veinlets that cut massive pyrrhotite + pyrite + chalcopyrite (Fig. 10f). Quartz is abundant as discrete grains interstitial to sulfides and commonly is intergrown with carbonate. Hisingerite [$\text{Fe}_7\text{Si}_2\text{O}_5(\text{OH})_4 \cdot 2\text{H}_2\text{O}$] is an amber to dark brown, conchoidally fracturing mineral that forms anastomosing or horsetail veinlets cutting massive sulfide in the SSB. The mineral postdates deformation and metamorphism because the veinlets themselves are undeformed and randomly cut massive sulfide. Stilpnomelane occurs as fibrous intergrowths with pyrrhotite, chalcopyrite, chlorite, and quartz within sulfide masses. In thin section, it varies from brownish green to orange brown. Chlorite is present within massive sulfide as overgrowths on sulfides. It forms well-crystallized hexagonal books, fine-grained randomly intergrown fibers, and very fine-grained mats. McCarthy and Robinson (1991) noted the occurrence of trace barite in the western periphery of the SSB.

Pyrite is generally the first sulfide to have been deposited and, in places, good evidence exists that primary textures are preserved. Early pyrite is generally accompanied by siderite. Pyrrhotite, chalcopyrite, gold and electrum, marcasite, sphalerite, and digenite are interstitial to pyrite and may form overgrowths on pyrite. It is likely that these minerals were remobilized and recrystallized. The occurrence of magnetite as randomly oriented veinlets that cut deformation fabrics indicates that this mineral postdates deformation and metamorphism, and therefore is not primary. Within the stockwork zone, quartz precipitated in zones of intense silicification where the mineral pseudomorphs primary igneous minerals.

Primary textures found at Windy Craggy, particularly in the NSB, closely resemble those in weakly deformed and metamorphosed massive sulfide deposits. Besshi-type deposits rarely exhibit such textures due to their intense metamorphism and/or deformation. The textures at Windy Craggy are very similar to those in Cyprus-type deposits in Cyprus, Oman, Newfoundland, and Norway (e.g., Constantinou and Govett, 1973; Grenne and Vokes, 1990), and in the Kuroko-type deposits of Japan (e.g., Eldridge et al., 1983). Textural similarities are also shared with modern sea-floor sulfide deposits on non-sedimented (e.g., Oudin, 1983; Humphris et al., 1995) and sedimented spreading centers (e.g., Peter and Scott, 1988; Duckworth et al., 1994). The presence of euhedral pyrite is indicative of precipitation under stable hydrothermal conditions and suggests that the sulfide mass was very porous. In places, early colloform pyrite is a pseudomorph of chalcopyrite due to replacement by higher-temperature fluids. Some of the recrystallization of pyrite within massive mineralization may have taken place during the late stages of sulfide deposition as hydrothermal fluids circulated through a porous, preexisting sulfide mass. Hisingerite formed by supergene processes after deformation and metamorphism.

In the SSB, most mineral textures are the result of deformation and metamorphism. Examples of deformational textures include (1) quartz fibers developed on recrystallized pyrite cubes, reminiscent of the textures formed by crack-seal deformation (Ramsay, 1980), (2) deformation twin lamellae in pyrrhotite, (3) elongation of pyrrhotite crystals parallel to the direction of the penetrative deformation fabric, and (4) comminution of pyrite grains. Cataclasis appears to have involved brittle fracture, granulation, intragranular microfracture extension, and rotation of grains. Textures indicating brittle fracture of pyrite grains, together with infilling of extension microfractures with chalcopyrite and pyrrhotite, are consistent with cataclastic deformation of pyrite and mechanical or solution transfer of material into fractures.

Bulk Sulfide Chemistry

Mean metal contents and standard deviations (1σ) for the NSB are: 29.3 ± 8.6 wt percent Fe ($n = 793$); 1.2 ± 1.1 wt percent Cu ($n = 1,174$); 0.1 ± 0.05 wt percent Co ($n = 1,154$); 1.6 ± 2.6 g Ag/t ($n = 1,222$); 0.2 ± 0.3 g/t Au ($n = 1,262$); and for the SSB: 33.6 ± 10.9 wt percent Fe ($n = 447$); 1.3 ± 1.3 wt percent Cu ($n = 1,427$); 0.1 ± 0.05 wt percent Co ($n = 665$); 3.0 ± 5.7 g Ag/t ($n = 1,516$); 0.4 ± 1.5 g/t Au ($n = 1,538$) (unpublished data, Geddes Resources Ltd., 1990). Both the NSB and SSB are of similar size, but differences exist in their Zn contents. Portions of the NSB contain up to 5 wt percent Zn and concomitant anomalous concentrations of up to about 2 g/t Au. The SSB contains only local trace amounts of Zn. In the NSB, Zn correlates positively with Cd, As, Sb, Pb, Au, and Ag. High values of the above elements lack any correlation with Cu, Co, or Fe contents, and Co does not correlate well with Cu.

The relatively Zn-rich nature of the NSB may be due to precipitation of sphalerite from cooler hydrothermal

solutions (e.g., Large, 1977). This cannot be evaluated here because the SSB lens is too highly deformed for fluid inclusions to give meaningful results (Peter and Scott, 1993). The very low Pb content of the Windy Craggy massive sulfides is typical of ores within basaltic host rocks. Pelitic sediments are generally a good source of Pb; however, in this case they were not a significant contributor to the hydrothermal fluid. This is substantiated by sulfur isotope values of the sulfides (Peter and Scott, 1993), which indicate that the sulfur was probably derived overwhelmingly from basalt (see also below).

The average Co grade of proven and probable reserves at Windy Craggy is 0.082 wt percent yet no discrete Co-bearing phase, other than trace cobaltite that is associated with a late fault, has been identified. Some Co is present in pyrrhotite and pyrite, which electron microprobe analyses have shown to be compositionally highly variable and unzoned. Muir (1980) reported a pyrrhotite analysis of 0.29 wt percent Co and two analyses of pyrite containing 0.32 wt percent Co. Mainwaring (1983) analyzed pyrrhotite and pyrite from six Windy Craggy samples and found that pyrite contains from <0.03 to 3.2 wt percent Co (mean = 1 wt percent), and that coexisting pyrrhotite contains from <0.03 to 0.2 wt percent Co (mean = 0.1 wt percent). Mainwaring (1983) determined that most of the pyrite enclosed in pyrrhotite is richer in Co than the pyrite enclosed in gangue or chalcopyrite. Where both euhedral and framboidal pyrite occur in the same specimen, the framboidal variety generally has more Co. Besshi-type ores contain Co from several hundred to several thousand ppm Co with a mean of 1,000 ppm (Itoh, 1976). Pyrrhotite in the Besshi mine contains up to 2,000 ppm Co (Kase and Yamamoto, 1988), and Co-rich pentlandite, Co-bearing mackinawite, and cobaltite have been noted at the Shimokawa deposit (Bamba and Motoyoshi, 1985). The presence of significant Co at Windy Craggy is intriguing, as the element is not generally concentrated in hydrothermal solutions. However, according to Crerar et al. (1985), the solubility of Co is enhanced by high temperature and high salinity.

The average Au content of massive sulfide at Windy Craggy is 0.22 ppm. The exhalite at Windy Craggy typically is not auriferous, although in several places it contains anomalous values between 1 and 10 g/t Au. A zone of significant Au enrichment was intersected at the margin of the SSB in several drill holes. This Au-bearing zone contains fine-grained, mottled sulfide and a carbonate together comprising intergrown pyrite, pyrrhotite, chalcopyrite, magnetite, brown-gray siderite, and milky white calcite fragments and bands or beds of milky white, cryptocrystalline quartz; less common are clasts of fine-grained mafic volcanic rock and fragments of laminated to banded argillite. Rare discrete grains of visible gold 30 to 80 μm in diameter are associated with sulfides and carbonates. By comparison, little is known of the distribution of precious metals in Japanese Besshi-type deposits. Native gold is recorded as minute grains in the Okuki, Sekizen, and Yokei deposits (Horikoshi, 1959; Takeda and Sekine, 1960; Tsunori, 1962). Maeda et al. (1981) reported the occurrence of electrum in the Shimokawa mine, Hokkaido; this

deposit has many similarities with Windy Craggy and is situated at the boundary between diabase and phyllite. At Shimokawa, electrum occurs as irregular <30 μm diameter grains associated with sphalerite and pyrrhotite.

Basalt Geochemistry

Immobile trace and rare earth element geochemistry is utilized here to deduce the tectonic setting of the Windy Craggy deposit. Information from geologic relationships is of limited value because of the allochthonous nature of the Alexander terrane. Major element abundances are also of limited use, as some of them (especially alkalis) are susceptible to modification during hydrothermal alteration and low-grade regional metamorphism. The alteration of most Windy Craggy samples is appreciable, as indicated by high H_2O and CO_2 , and low Na_2O and K_2O contents, particularly in the stratigraphic hanging wall of the deposit. Furthermore, there has been iron enrichment associated with mineralization (Fig. 11a). Data for sills intercalated with footwall argillite plot distinctly within the calc-alkaline field of Figure 11a, whereas those for footwall and hanging wall flows plot predominantly in the tholeiitic field, showing varying degrees of iron enrichment. This is an artifact accompanying alteration superposed on the primary compositions, as the sill samples were collected much farther from the deposit and are commonly less altered than the proximal flows. A transitional magma series is suggested because data for the least altered samples plot on either side of the calc-alkaline-tholeiitic boundary.

On an $\text{Na}_2\text{O} + \text{K}_2\text{O}$ vs. SiO_2 plot (Fig. 11b) of Irvine and Baragar (1971), data for the sills fall predominantly within the alkaline field, with some on the dividing line. Most of the flow samples are within the subalkaline field, although some of the hanging-wall samples are within the alkaline field. A number of the samples display a severe depletion of Na and K due to hydrothermal alteration.

Positive interelement correlations among Zr, Ti, and P and among MgO, Cr, and Ni, as well as constant ratios of high field strength elements (HFSE) Zr/Hf (~39) and Nb/Ta (~16) indicate that these elements have not been significantly mobilized during hydrothermal alteration. On a $\log(\text{Zr}/\text{TiO}_2)$ vs. $\log(\text{Nb}/\text{Y})$ plot of Winchester and Floyd (1977), data for most of the Windy Craggy basaltic host rocks (except cutting dikes) plot within the alkaline basalt field (Fig. 11c). This diagram clearly distinguishes later, crosscutting dikes from the flows and sills, with the former plotting in the andesite/basalt and sub-alkaline basalt fields.

The Hf-Th-Ta ternary plot of Wood (1980) is extremely useful in discriminating the Windy Craggy basalts (Fig. 11d) because Th is immobile under greenschist-facies metamorphic conditions. Furthermore, Th and Ta behave coherently in non subduction-related oceanic basalts, decoupling only in the subduction environment (Wood, 1980). All of the flow and sill samples plot in the field of alkaline, within-plate basalt (WPB), except for a few samples that plot in the field of enriched mid-ocean ridge basalt (E-MORB). Dikes plot in the volcanic-arc basalt (VAB) field. Flows and sills also plot in the within-plate alkaline basalt (WPA) fields on the Zr-Nb-Y ternary plot

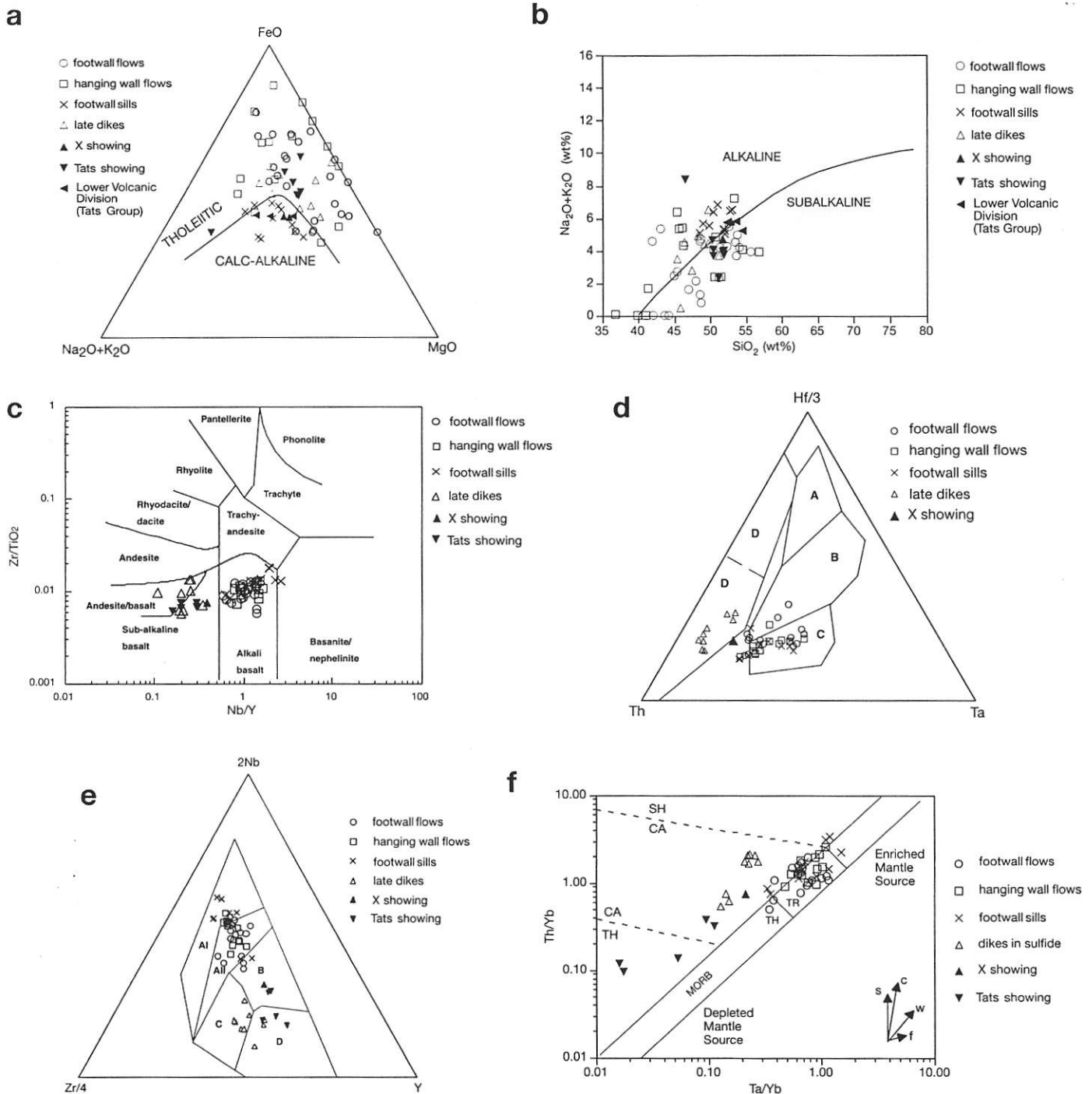


FIG. 11. a. AFM plot showing calc-alkaline and tholeiitic fields (Irvine and Baragar, 1971) and Fe-enrichment for Windy Craggy basaltic rock samples; b. Plot of SiO_2 versus $\text{Na}_2\text{O} + \text{K}_2\text{O}$ for igneous rocks showing alkaline and subalkaline fields of Irvine and Baragar (1971); c. $\text{Log}(\text{Nb}/\text{Y})$ versus $\text{Log}(\text{Zr}/\text{TiO}_2)$ plot of Winchester and Floyd (1977) showing alkaline nature of Windy Craggy footwall and hanging wall basalt flows and sills; d. $\text{Hf}/3$ - Th - Ta ternary plot of Wood (1980) showing fields for N-MORB (A), E-MORB (B), alkaline within-plate basalts (C), and volcanic arc basalts (D); e. 2Nb - $\text{Zr}/4$ - Y ternary plot of Meschede (1986) showing fields for within-plate alkaline basalt (AI, AII), within-plate tholeiite (AII, C), plume-type mid-ocean ridge basalt (B), normal mid-ocean ridge basalt (D), and volcanic arc basalt (C, D); f. $\text{Log}(\text{Ta}/\text{Yb})$ versus $\text{Log}(\text{Th}/\text{Yb})$ plot of Pearce (1983) showing distinction between flows and sills versus dikes that cut sulfide mineralization. TH = tholeiitic, CA = calc-alkaline, SH = shoshonitic, TR = transitional, ALK = alkaline. Vectors shown indicate the influence of different components and processes: s = subduction zone enrichment; c = crustal contamination; w = within-plate enrichment; f = fractional crystallization (for $F = 0.5$). Within-plate magmatism enriches Ta and Th equally, and individual samples plot along a vector (w) with a slope of unity. In subduction-related rocks, however, only Th is affected, and the resultant vector (s) is subvertical; during crustal contamination Th is affected to a far greater degree than Ta, and its vector (c) is also subvertical. The flows and sills are derived from enriched mantle sources, whereas the later dikes which cut sulfides show a subduction or crustal contamination influence from a less-enriched mantle source.

(Fig. 11e) of Meschede (1986), whereas the dikes lie in the volcanic-arc basalt (VAB) fields.

Figure 11f is a Th/Yb vs. Ta/Yb plot of Pearce (1983). The normalizing factor Yb is effective in largely eliminating variations due to partial melting and fractional crystallization. Vectors on the diagram illustrate the relative effects of certain igneous processes on the primary geochemical composition of a particular suite of basalts. Windy Craggy basaltic rocks plot along the "mantle array,"

suggesting that the mantle source of the basalts was not influenced by subduction-related fluids and the magmas were not significantly affected by crustal contamination. This figure illustrates the transitional nature of the flows and sills, and clearly distinguishes these from the late dikes that plot in the calc-alkaline field.

Figure 12a-f shows MORB-normalized geochemical patterns (spider diagrams) arranged in order of increasing element compatibility, with the most incompatible elements

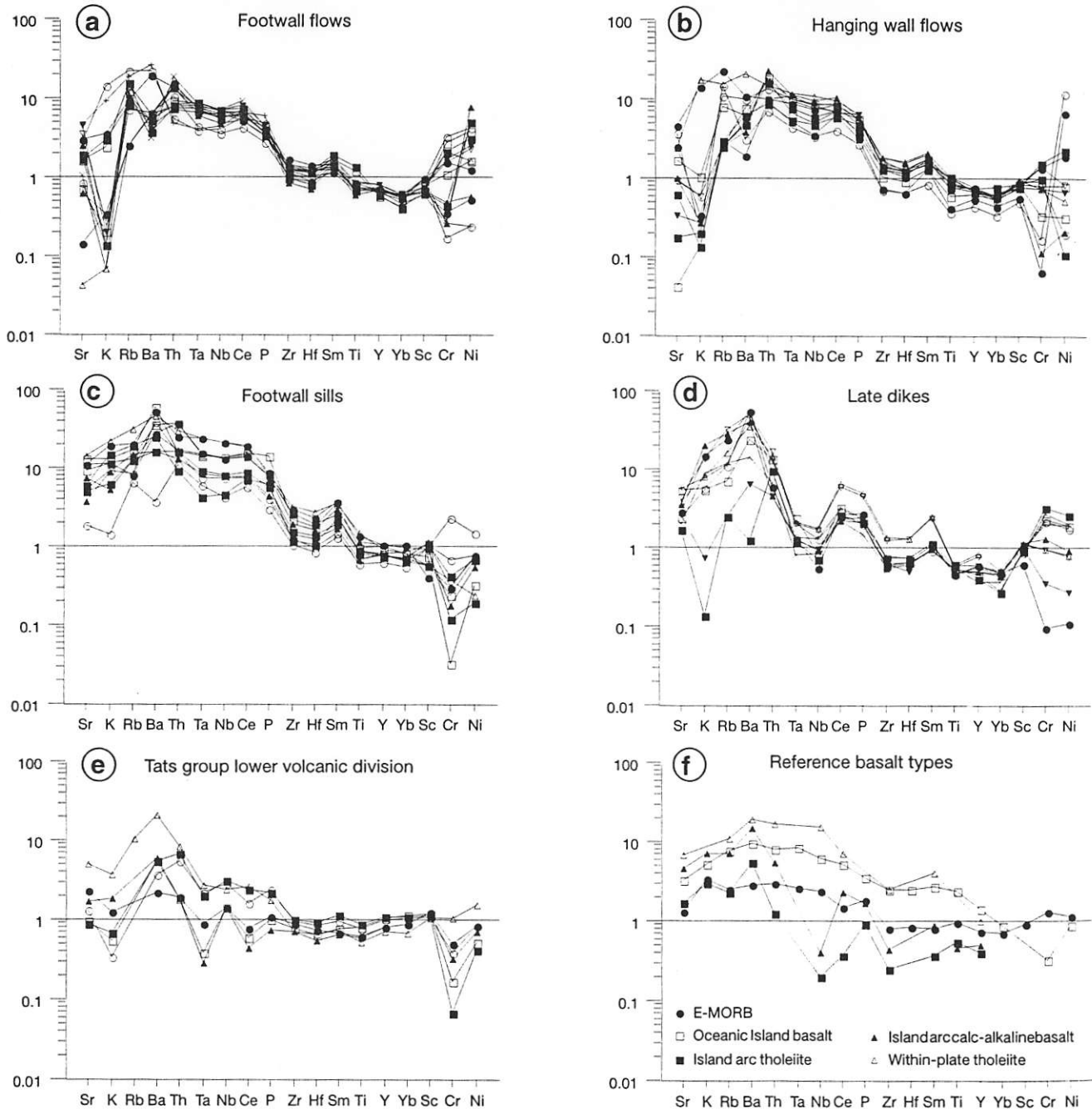


FIG. 12. Spider diagram of Windy Craggy igneous host rocks normalized to MORB (Pearce, 1983): a. footwall flows; b. hanging wall flows; c. footwall sills; d. late dikes; e. Tats group lower volcanic division basalts (data from Smith and Fox, 1989a, b.); and f. reference basalt types: average mid-ocean ridge basalt (Sun, 1980; Sun et al., 1979), typical Hawaiian tholeiite (Chen and Frey, 1983), alkali basalt (Chen and Frey, 1983), average continental alkali basalt from Kenya (Baker et al., 1977), average island arc calc-alkaline basalt (Sun et al., 1979), and average arc tholeiite (Sun et al., 1979).

plotted on the left. The shape of patterns on such plots is little-affected by differences in partial melting and fractional crystallization (Pearce, 1983); therefore, variations among the patterns are best explained in terms of heterogeneities in mantle sources. The main incompatible element-depleted reservoir of convecting upper mantle is thought to yield flat patterns of normal mid-ocean ridge basalt (N-MORB), whereas the humped patterns are believed to be derived from incompatible element-enriched portions of this reservoir, such as those associated with "mantle plumes" (e.g., Tarney et al., 1980). Figure 12f shows reference patterns for a variety of basalt types (see figure caption). Both types of island arc basalt are characteristically enriched in K, Ba, Sr, and Rb and depleted in Ta, Nb, and Ti (weakly), relative to adjacent elements in the spider diagram. The late dikes from Windy Craggy (Fig. 12d), are distinct from all other units (Figs. 12a-c). These dikes also show LILE-enrichments but are depleted in Ta and Nb, with respect to adjacent elements. Similarities in the patterns for the Windy Craggy sills and flows (Figs. 12a-c) suggest that they are derived from a common magma source.

Figure 13a-f displays chondrite-normalized REE abundance patterns for Windy Craggy basaltic rocks and basalts of known tectonic setting for reference. The patterns for the basalts that host the Windy Craggy deposit show significant variation from moderate to steep LREE enrichment, with $(La/Yb)_n$ ranging from 7.1 to 25.4. Most of the basalts lack significant Eu anomalies, implying that little or no plagioclase fractionation occurred during magmatic processes. For some samples, there also is a tendency for the HREE portion of the pattern, from Tb to Yb, to cross over, suggesting that garnet was residual in the mantle source during initial generation of the basaltic melts (Green, 1973). This requires that the magmas were generated at pressures greater than 20 kbar (depths >75 km), which is the minimum pressure required for garnet stability.

The Windy Craggy flows and sills are more LILE- and LREE-enriched than E-MORB or transitional mid-ocean ridge basalts (T-MORB) (Schilling et al., 1983) and in this respect are similar to continental flood basalts, oceanic transform basalts (Batiza and Vanko, 1985; Shibata et al., 1979), oceanic island alkali basalts (Sun, 1980), and calc-alkaline island arc basalts (Sun, 1980). Transitional to alkaline volcanics from the submerged parts of ocean basins have been described by several investigators (e.g., Aumento, 1968; Stebbins and Thompson, 1978). Such volcanic rocks have been found close to continents and have been related to the initial stages of back-arc spreading or back-arc rifting, e.g., Penguin Island (Weaver et al., 1979) and in southern Chile (Saunders et al., 1979). The pronounced LILE- and LREE-enriched nature of the Windy Craggy volcanics argues convincingly against a setting along a typical mid-ocean spreading ridge. Such sites are characterized by basalts of depleted N-MORB composition. The geochemistry of Windy Craggy flows and sills is most similar to that of mildly alkalic, within-plate tholeiites.

Low degrees of partial melting within the mantle are hypothesized to give rise to alkalic melts enriched in

incompatible minor and trace elements such as those at Windy Craggy (e.g., Ahern and Turcotte, 1979). This hypothesis has been applied to oceanic intra-plate magmas (e.g., Wright, 1984). The initial stages of thermal disturbance that ultimately result in active sea-floor spreading should be marked by relatively low degrees of melting which, if the mantle melting were an Hawaiian pyrolite-type lithosphere, would generate alkalic melts. As mantle upwelling continues beneath a developing ridge, diapirs of asthenosphere-derived (MORB-pyrolite) mantle are progressively more important magma sources.

Lower Tats Volcanics: The "Arc Connection"

A hallmark characteristic of basalts formed in arc environments is their ubiquitous depletions in the high field strength elements (HFSE) Ti, Ta, Nb, Y (Fig. 12f) (e.g., Pearce, 1983). Footwall basalt flows and sills at Windy Craggy lack HFSE depletions that are characteristic of arc-derived volcanics (Fig. 12a-c) and, on this basis, an arc-related setting for the Windy Craggy basalt flows and sills is ruled out. However, the samples used in this study are from a relatively restricted area in and around the deposit, hence the lack of an "arc signature" at Windy Craggy, other than for the late dikes, may relate to spatial heterogeneities in mantle chemistry or to temporal geochemical effects related to rifting.

The geochemistry of stratigraphically equivalent and non-alkalic basalts from the nearby Tats and X Showings are illustrated in several of the plots in Figure 11. Figure 13e shows that these basalts have chondrite-normalized REE patterns that range from depleted N-MORB, through non-LREE depleted, to E-MORB. For the Tats Showing basalts, $(La/Yb)_n$ ratios range from 0.4 to 2.1 and all samples display variable Eu depletions indicative of plagioclase crystallization. Figure 12e, a spider diagram of the Tats and X Showing basalts, indicates mild LILE enrichment, albeit less pronounced than that displayed by the Windy Craggy basalts. A salient feature of this diagram is the variable depletion of Ta relative to adjacent Th for the Tats Showing basalts.

Ta-Nb troughs displayed by the LVD basalts are characteristic of arc environments (Pearce, 1983). Because the LVD and MVD are approximately coeval, this indicates that the Windy Craggy basalt flows and sills (and LVD) likely formed in the vicinity of a volcanic arc, or from melts that were influenced to varying degrees by subducted oceanic crust. Such a scenario is consistent with a back-arc setting, where back-arc basin basalts (BABB) with negative Ta anomalies are restricted to those basins that form behind a well-developed island arc. This is discussed more fully below.

Detrital and Chemical Sediment Geochemistry

Major, trace, and REE geochemical data for fine-grained calcareous to non-calcareous argillites and exhalites that host the Windy Craggy deposit also provide information on provenance, tectonic setting, and relative input from clastic, hydrothermal, and hydrogenous sources. Argillite is dominated by SiO_2 , Al_2O_3 , Fe_2O_3 , MgO, CaO, and CO_2 ,

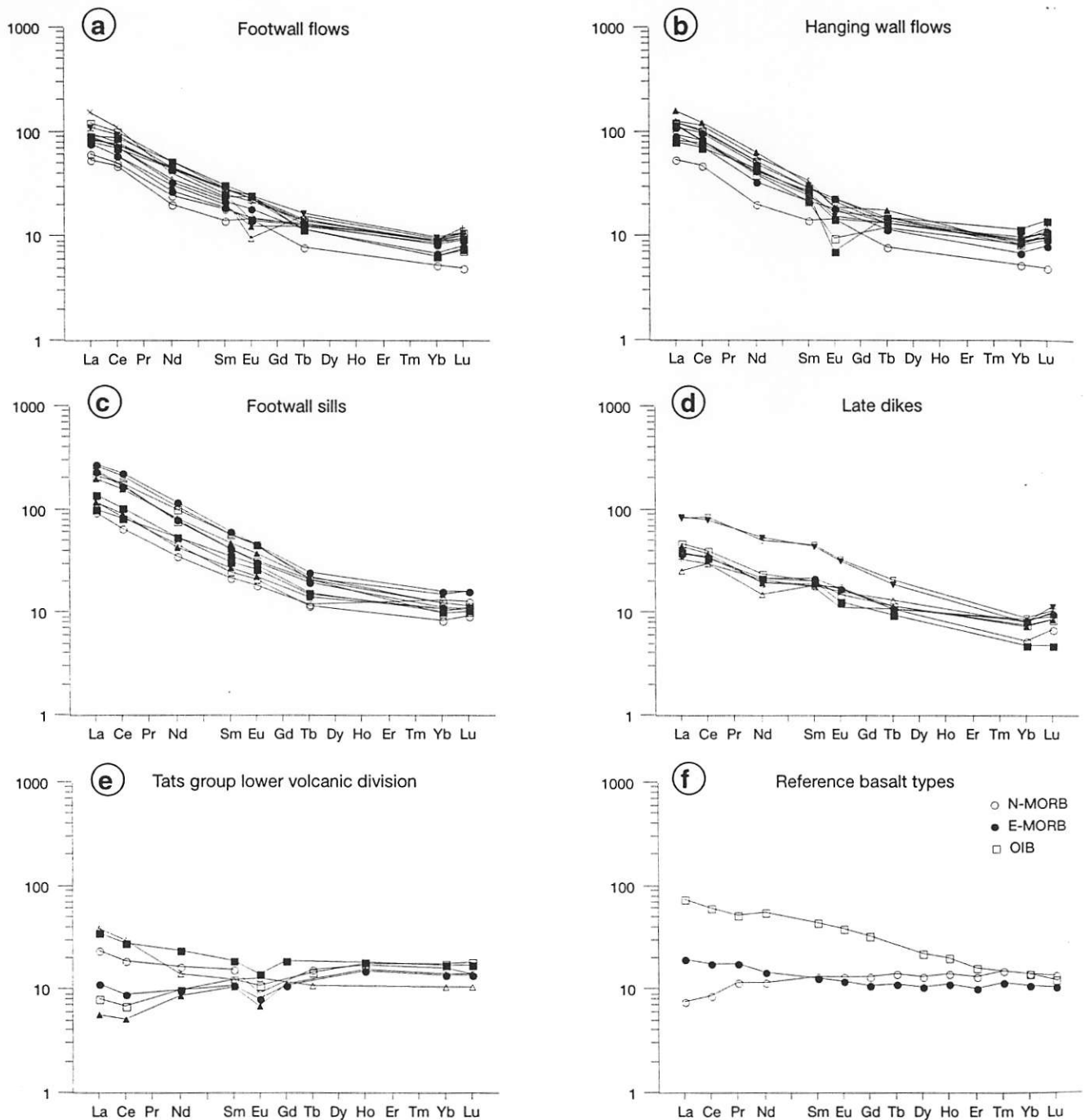


FIG. 13. Chondrite normalized (Rock, 1988) rare earth element plot for Windy Craggy igneous host rocks: a. footwall flows; b. hanging-wall flows; c. footwall sills; d. late dikes; e. Tats group lower volcanic division basalts (Smith and Fox, 1989a, b); and f. reference basalt types: average mid-ocean ridge basalt (N-MORB), typical E-MORB, and oceanic island basalt (OIB) (Sun, 1980; Sun et al., 1979).

with minor TiO_2 , MnO , Na_2O , H_2O , and S. Compared to the North American shale composite (NASC) of Gromet et al. (1984), most of the Windy Craggy argillite samples are depleted in TiO_2 , Al_2O_3 , and K_2O , and are enriched with respect to Fe_2O_3 , MnO , MgO , and P_2O_5 ; some samples are also enriched in CaO and Na_2O . All of the samples display marked positive correlations between Al_2O_3 and TiO_2 ($r = +0.948$). Although mudrocks commonly have high

K_2O contents because of the presence of abundant clay minerals, Windy Craggy argillite generally has <0.5 wt percent K_2O ; this probably reflects the removal of K by hydrothermal alteration. LILE element (e.g., K, Rb, Cs, Sr, La, Th, and U) abundances are variable, although specific element ratios are approximately constant. The transition trace elements (Ni, Cr, V, Sc) exhibit near constant inter-element ratios. The HFSE, Ti, Zr, Y, Nb, and Hf do not uniformly

show consistent inter-element relations as their distributions are partly governed by their relative abundance in heavy minerals. The Windy Craggy exhalite samples are dominated by SiO_2 , Fe_2O_3 , CaO , CO_2 , and S, with minor MnO , MgO , and P_2O_5 . Mn/Fe ratios for exhalites are all less than 0.1, and are much lower than those for modern East Pacific Rise metalliferous sediment (Dymond et al., 1977).

The relative proportions of Al, Fe, and Mn in marine sediments are a measure of the hydrothermal contribution to the sediments (Boström, 1973). Figure 14 is an Al-Fe-Mn plot for Windy Craggy unaltered footwall and hanging-wall argillite and exhalite samples showing, for comparison, the fields for hydrothermal and non-hydrothermal sediments and other recent and ancient exhalites. Most of the Windy Craggy exhalite samples are more Fe-rich and Al-poor (at similar relative Mn contents) than the argillite samples, and fall in the hydrothermal field defined by compositions of modern hydrothermal metalliferous sediments. Some Windy Craggy argillites fall in the hydrothermal field, but they also extend to the non-hydrothermal field. This pattern suggests that an appreciable hydrothermal component is present in many of the Windy Craggy argillite samples.

In order to determine the relative contributions of terrigenous clastic (Al, Ti) and hydrothermal (Fe, Mn) components within metalliferous and pelagic sediments, Boström (1973) developed a Fe/Ti versus Al/(Al + Fe + Mn) plot, shown here in Figure 15. The plot includes data for Windy Craggy unaltered footwall and hanging-wall argillites, exhalites, and unaltered Windy Craggy basaltic sills and

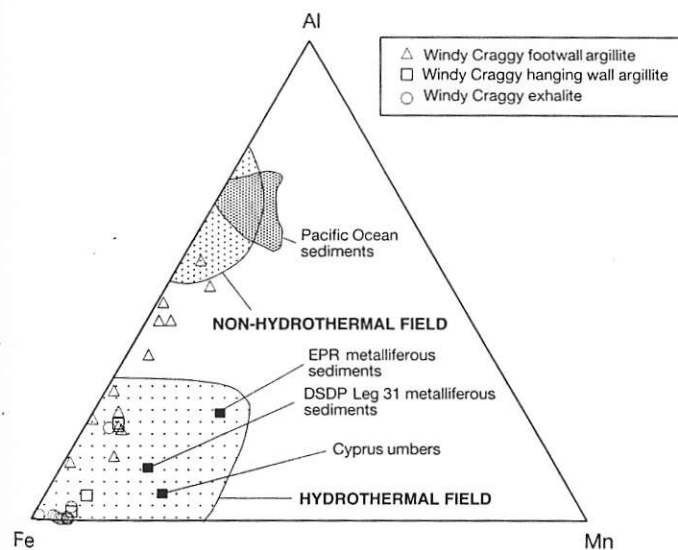


FIG. 14. Al-Fe-Mn ternary diagram of Boström (1973) showing data for Windy Craggy unaltered footwall and hanging wall argillite and exhalite samples, and fields for hydrothermal and non-hydrothermal deposits. Also shown are other exhalites and metalliferous sediments for comparison: (1) East Pacific Rise (EPR) deposits, field III (Boström, 1973); (2) basal metalliferous sediments from DSDP Leg 31, Site 294, core 6 (average of 4 samples; Bonatti et al., 1979); (3) Cyprus umbers overlying pillow lavas of the Troodos massif (average of 23 samples; Robertson and Hudson, 1973); (4) East Pacific Rise deposits from station Amph D2 in the southern Pacific Ocean (average of 3 samples; Bonatti and Joensuu, 1966); and (5) East Pacific Rise deposits, group b (average of 9 samples; Boström and Peterson, 1969).

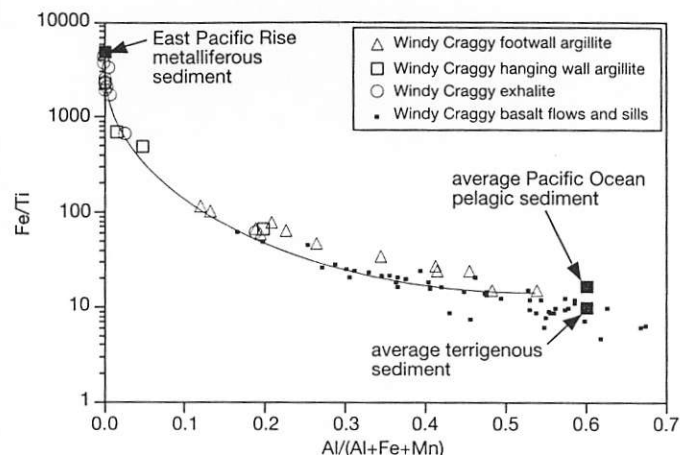


FIG. 15. Al/(Al + Fe + Mn) versus Fe/Ti diagram for Windy Craggy unaltered footwall and hanging wall argillite and exhalite samples, and for reference, Windy Craggy unaltered basalt flows and sills (Peter and Scott, 1990). Also shown are fields for (1) East Pacific Rise modern metalliferous sediments (Boström, 1980); (2) average Pacific Ocean pelagic sediment (Boström, 1983); and (3) average terrigenous sediment (Boström, 1970).

flows (from Peter and Scott, 1990). Also shown are average pelagic Pacific Ocean sediment, average terrigenous sediment, and East Pacific Rise (EPR) modern metalliferous sediment. Analyses of Windy Craggy argillite define a continuous mixing curve between relatively pure metalliferous sediment and Windy Craggy basalts; all but two of the Windy Craggy exhalites plot very close to the end-member composition for the metalliferous sediments.

NASC-normalized (Gromet et al., 1984) REE patterns for Windy Craggy argillite, determined on a carbonate- and H_2O -free basis, are shown in Fig. 16a-c. Windy Craggy argillite contains much lower LREE and slightly lower HREE (Fig. 16a-c), than the NASC, which is considered to reflect the average composition of the continental source material (upper crust); $(\text{La}/\text{Yb})_{\text{NASC}}$ ratios range from 0.42 to 0.92. All of the patterns show slightly to strongly negative Ce anomalies, and both positive and negative Eu anomalies. Except for their pronounced negative Ce anomalies, REE patterns for the Windy Craggy argillite are very similar to those of recent muds from back-arc basins in the southwest Pacific, Bering Sea, and Japan, and also from continental arcs (McLennan et al., 1990).

Figure 16d shows that chondrite-normalized REE patterns of Windy Craggy exhalites are surprisingly variable, although there is little variability within a single exhalite unit. The patterns range from strong enrichment in LREE and strongly to moderately positive Eu anomalies, to moderate enrichment in LREE and moderately negative Ce anomalies. REE abundances for most samples are far less than those of NASC (Gromet et al., 1984) and the Windy Craggy argillite (Fig. 16a-c). The distinctive depletions in Ce are characteristic of most seawater (e.g., Hogdahl et al., 1968), marine carbonate (e.g., Parekh et al., 1977), foram tests (Palmer, 1985), modern pelagic clays (e.g., Shaw and Wasserburg, 1985), and modern metalliferous sediments

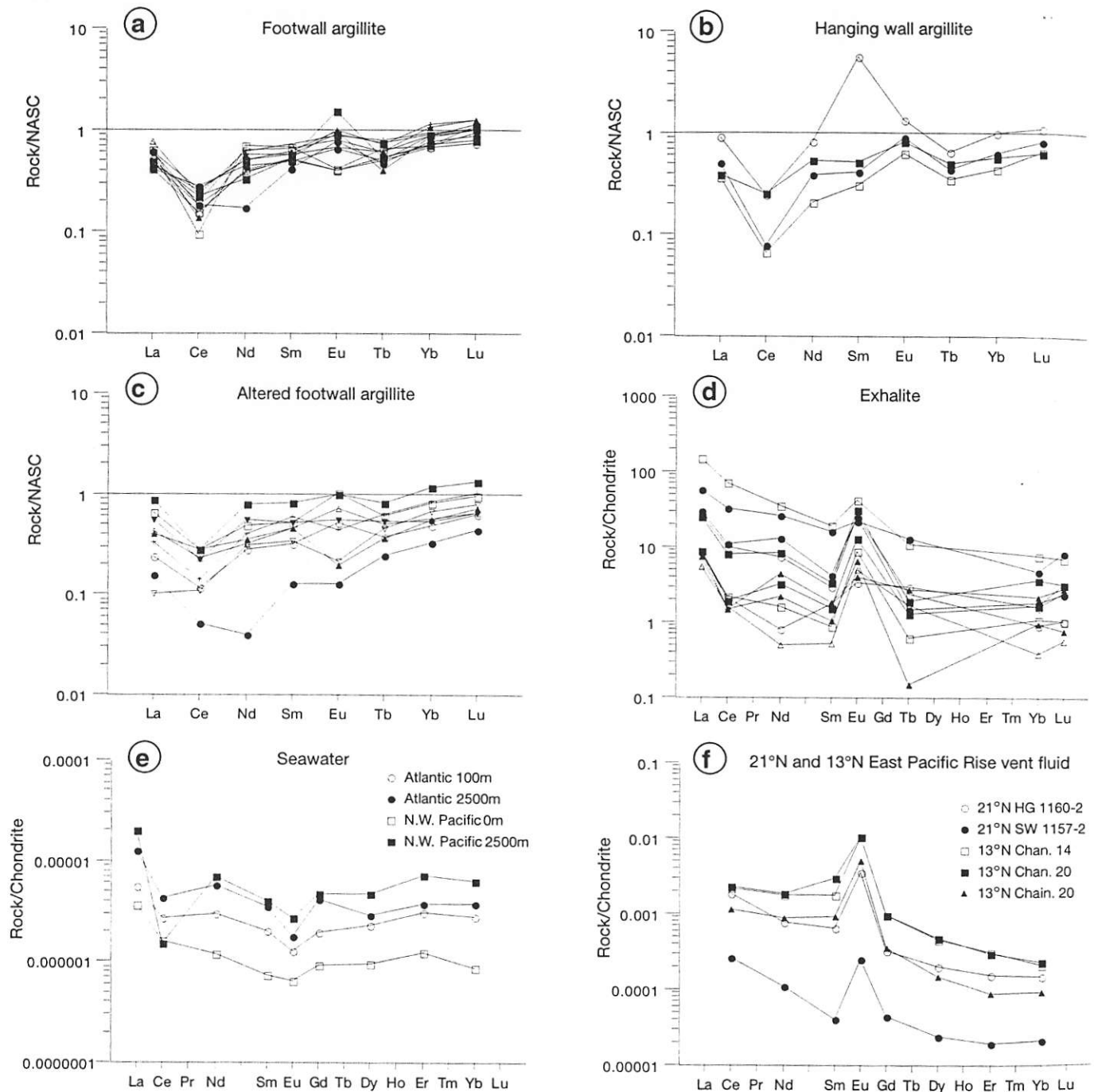


FIG. 16. North American Shale Composite (NASC) and chondrite-normalized rare earth element patterns for: a. Windy Craggy footwall argillite; b. Windy Craggy hanging-wall argillite; c. Windy Craggy altered footwall argillite; d. Windy Craggy exhalite; e. surface and deep Atlantic and Pacific seawater (Hogdahl et al., 1968); and f. hydrothermal vent fluids from 21° and 13°N, East Pacific Rise (Michard and Albarède, 1986). NASC data from Gromet et al. (1984); chondrite data from Rock (1988).

(e.g., Piper and Graef, 1974). Authigenic sediments accurately reflect the relative Ce abundances of the waters from which they formed (e.g., Shimizu and Masuda, 1977).

Some Windy Craggy argillite samples display negative Eu anomalies similar to those of NASC, whereas others lack Eu anomalies or have a positive anomaly (Fig. 16a-c). Slightly to moderately positive Eu anomalies in several samples

may result from plagioclase enrichment or hydrothermal minerals such as carbonate. The REE characteristics of Windy Craggy argillite are similar to those of modern turbidites of the northwest Atlantic Ocean (Addy, 1979), deeply buried Gulf Coast sediments (Chaudhuri and Cullers, 1979), and other platform and cratonic sedimentary rocks (e.g., Cullers et al., 1979).

The discovery of submarine hydrothermal plumes that vent fine-grained sulfide particles (pyrrhotite, sphalerite, pyrite, chalcopyrite), amorphous silica, and anhydrite (e.g., Mottl and McConachy, 1990) provides a modern analog for ancient exhalites. Barrett et al. (1990) reported REE patterns for modern massive sulfide-sulfate-silica samples from the Southern Explorer Ridge that are similar to those of the Windy Craggy exhalites. Windy Craggy samples that have large positive Eu anomalies are similar to those of 350°C hydrothermal fluids discharging from modern black smokers (Fig. 16f). The similarity of REE patterns for Windy Craggy exhalites and EPR vent fluids, and differences in REE chemistries of the basalts at these two sites, indicate that the REE patterns of hydrothermal vent fluids are not controlled by the composition of the host rocks.

Metal contents of the Windy Craggy exhalite samples vary widely: Cu (31–12,400 ppm; mean 3,426); Pb (7–375 ppm; mean 76); Zn (79–844 ppm; mean 276); As (1.5–419 ppm; mean 77); and Sb (1.5–43 ppm; mean 10). Exhalites also contain elevated values of Bi, Mo, and Ni. Windy Craggy exhalites are not typically auriferous (2–298 ppb; mean 57 ppb), although in several places they contain high values between 1 and 10 ppm Au (Peter, 1989). The sample having the highest Au also has the highest Fe and the second highest Mn content. This suggests that Au is genetically related to the hydrothermal exhalative component (Fe and Mn), as proposed by Boström (1970).

A Back-Arc Setting for the Windy Craggy Deposit

In the Alexander terrane, felsic volcanic rocks occur in predominantly mafic volcanic sections and indicate that volcanism in the terrane was regionally bimodal. However, such felsic volcanic rocks or their metamorphosed equivalents are absent from the mafic volcanic sequence in the Windy Craggy area (MacIntyre, 1984). MacIntyre (1986) proposed that the Windy Craggy deposit formed in a back-arc basin on continental crust and that the rectilinear nature of the faults bounding Triassic rocks in the Windy Craggy area reflects compression of an earlier pull-apart basin that may have been located on a transcurrent fault system. Dawson (1990) suggested that the Upper Triassic Windy Craggy host rocks formed as a result of epicontinental rifting subsequent to amalgamation with Wrangellia in Carboniferous time, and prior to collision between the Insular Superterrane and North America in the Cretaceous. He based this conclusion, in part, on the presence of adjacent miogeoclinal sediments, the geographical progression from tholeiitic to calc-alkaline volcanics, and the presence of turbiditic clastic rocks. The presence of only minor tuff beds indicates that Windy Craggy did not form in proximity to a well-developed island arc, and together with the absence of coarse-grained turbiditic sediments, this suggests deposition in a mature back-arc basin, far from a sediment source (Klein, 1975a, b).

Back-arc basin basalts (BABB), a distinct magma type characteristic of back-arc basins, are enriched in volatiles and other incompatible elements. They have higher abundances

of LILE (Ba, Rb, K, Sr) and LREE than are observed in normal MORB (e.g., Fryer et al., 1981). Sinton and Fryer (1987) proposed a complex model by which BABB are generated during hydrous partial melting of a depleted lithospheric source that has undergone enrichment in incompatible minor and trace elements prior to melting. They suggested that the enrichment process is related to migration of fluids and melt derived from subducted lithosphere beneath the back-arc basin. LILE and LREE-enriched basalts having similar trace and REE compositions to those at Windy Craggy (i.e., lacking an arc signature) occur in back arc environments on the South Pandora Ridge (Price et al., 1990), and on the Fiji Fracture Zone of the North Fiji Basin (Johnson and Sinton, 1990).

Sm and Nd isotope data for Windy Craggy basalts (Smith and Fox, 1989a, b) yield ϵ_{Nd} (at 220 Ma) values between +2.4 and +3.6. Such values can arise from the melting of an enriched mantle source or by mixing/incorporating a very small amount of continental crust with a depleted mantle source. The Windy Craggy values are within the range for BABB and rocks from continental-margin arcs (-4 to +10) but exclude N-MORBs (+8 to +12), intraoceanic-arc rocks (+6 to +10), island-arc rocks (+6 to +10), OIBs (+4.5 to +6), and alkali basalts (+4.5 to +6.2). ϵ_{Nd} values for the Tats Showing basalts (LVD) range between +5.5 and +7.8 (Smith and Fox, 1989a, b) and overlap the field for typical primitive island arcs. Samson et al. (1989) conducted a Sm-Nd and Rb-Sr isotope study of the Alexander terrane, and concluded that it is composed of juvenile, mantle-derived material (rather than reworked crust) and probably formed in an intraoceanic, volcanic arc setting.

Important differences exist in the Pb-isotope geochemistry of basalts from different tectonic settings (e.g., Sun, 1980). In general, the lead isotope composition of OIB is more radiogenic and variable than that of typical MORB. Windy Craggy basalt and argillite samples define a linear trend on a $^{207}\text{Pb}/^{204}\text{Pb}$ versus $^{206}\text{Pb}/^{204}\text{Pb}$ plot, extending from a least radiogenic point defined by an intermediate value for Windy Craggy sulfides (Fig. 17). This least radiogenic point ($^{206}\text{Pb}/^{204}\text{Pb} = 18.70$, $^{208}\text{Pb}/^{204}\text{Pb} = 38.35$, and $^{207}\text{Pb}/^{204}\text{Pb} = 15.585$; Peter and Scott, 1990), which is interpreted to be the initial ratio for these rocks, lies just outside the MORB field but is within the fields for OIB as well as oceanic island arc basalt (IAB) (e.g., Mariana arc) and continental tholeiites. Bulk U and Th analyses support the conclusion that the linear trend for the host rocks shown in Figure 17 is due to in situ radiogenic growth since the time of mineralization. This linearity indicates that the sedimentary rocks inherited their initial Pb isotope compositions from precursor mafic volcanic rocks. The most likely source for these volcanic rocks is the arc itself, as LREE-enriched arc basalts have the required precursor compositions.

Plots involving La, Th, Sc, Co, and Zr can be used to distinguish sediments derived from oceanic island arcs, continental island arcs, active continental margins, and passive margins (Bhatia and Crook, 1986). Application of

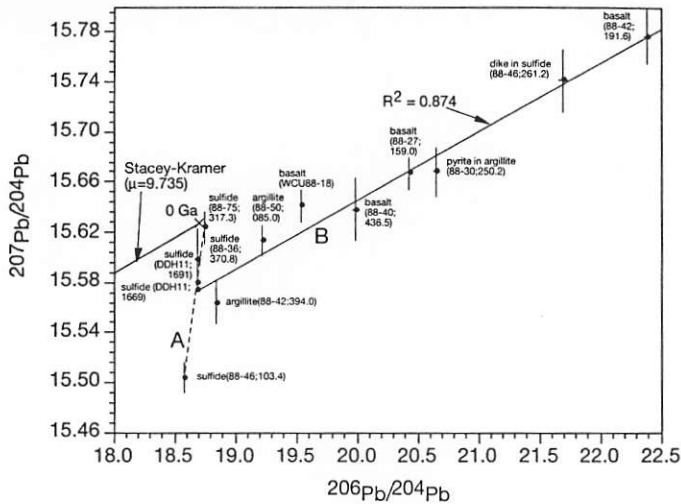


FIG. 17. $^{206}\text{Pb}/^{204}\text{Pb}$ versus $^{207}\text{Pb}/^{204}\text{Pb}$ plot for Windy Craggy sulfides, host rock argillite and basalt, and late dikes which cut sulfides. The growth curve of Stacey and Kramers (1975) is shown for reference.

such plots to the argillites in this study (Fig. 18a–c) suggest a Th-poor oceanic island arc and/or continental island arc setting, with Figure 18c unequivocally indicating that almost all of the samples fall in the former setting. For comparison, the shaded field is for Windy Craggy basalts, and the superposition of the argillite data on the basalt field, together with the argillite lead isotope compositions (see below), suggest that they were probably derived from eroded basalts of similar composition.

Ratios of certain trace elements in sedimentary rocks can also serve as indicators of tectonic setting (McLennan et al., 1990). Th/Sc ratios are particularly sensitive to average provenance composition because Th is highly incompatible and Sc is relatively compatible, and, as is the case for REEs (Taylor and McLennan, 1985), both elements are transferred quantitatively into terrigenous sediment during sedimentation. The Th/Sc ratio, therefore, provides a sensitive index of mafic versus felsic components. Th/Sc ratios for Windy Craggy argillite range from 0.06 to 0.17 (mean = 0.09), compared to ratios ~1.0 for most shales and upper crustal rocks, 0.17 for arc andesites, 0.05 for MORB, and >0.17 for felsic volcanic rocks (Taylor and McLennan, 1985). The low Th/Sc ratios of the Windy Craggy argillites thus record a significant mafic volcanic component. Collectively, the trace element geochemical evidence for the Windy Craggy argillites indicate that these sediments were not derived from a continental land mass.

The trace element geochemical characteristics of the Windy Craggy basalt flows and sills are consistent with their derivation from an enriched mantle source. The presence of MORB in the stratigraphic sequence in the Windy Craggy area suggests that the mantle beneath Windy Craggy was heterogeneous (e.g., Hofmann, 1997). The basalt geochemical data are not inconsistent with derivation from a mantle plume; however, the lack of an extremely thick volcanic pile and the presence of abundant turbiditic argillites in the stratigraphic sequence at Windy

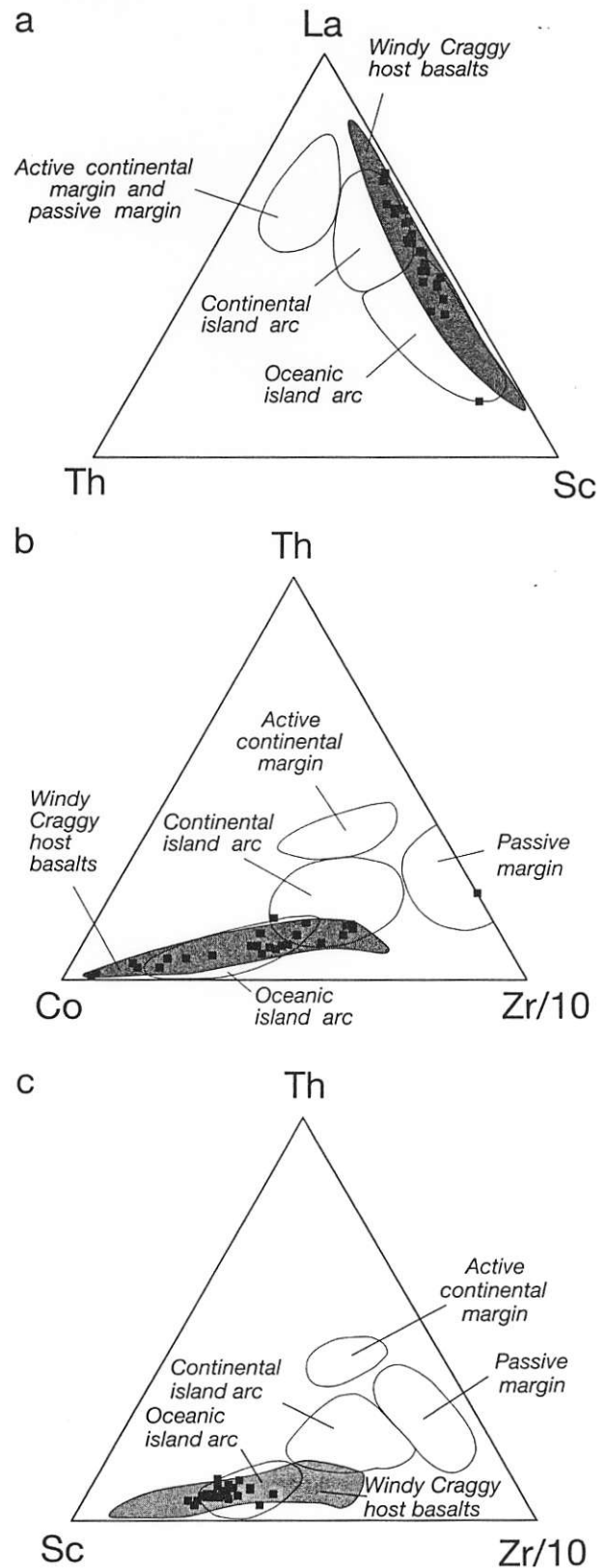


FIG. 18. Provenance discrimination plots of a. La-Th-Sc, b. Th-Co-Zr/10, and c. Th-Sc-Zr/10 (Bhatia and Crook, 1986) for Windy Craggy argillite samples (filled squares); also shown in gray are shaded fields for Windy Craggy basaltic sills and flows.

Craggy are inconsistent with an oceanic island setting. The Windy Craggy basalts are also similar to those formed in an incipient continental rift setting. However, the absence of felsic volcanic rocks in the stratigraphic succession at Windy Craggy, the trace element and REE compositions of the argillites (i.e., non-continental signature), the similarity of the Pb-isotope composition of the host argillites and basalts, and the Nd-isotope composition of the Alexander Terrane do not support such a setting. Based on juvenile Nd isotope signatures of various rock types, Samson et al. (1989) and Samson and Patchett (1991) suggested that the Terrane was not in proximity to a continental landmass prior to its accretion to North America. Collectively, the geologic relationships, basalt geochemical and Nd isotope data, argillite geochemical data suggest that the most likely tectonic setting for the mineralization was a back-arc basin.

Stratigraphic sequences in back-arc basins are extremely variable lithologically, and few general models exist. Juvenile or neo-formed back-arc basins contain a large amount of coarse grained clastics, including considerable volumes of volcanoclastic deep-water sediments (e.g., Cas and Wright, 1988). The absence of these deep water volcanoclastics in the Windy Craggy area suggests that its inferred back-arc basin setting must have been mature. Such a setting is also consistent with the presence of both LILE- and LREE-rich basalts without a subduction signature and N-MORB-type basalts having hallmark arc or subduction signatures in the Windy Craggy area. Late dikes that cut mineralization and all other lithologies are not volumetrically important within the local deposit area; however, they have geochemical signatures that relate to subduction processes that postdate formation of the footwall and hanging-wall basalts, and the deposit itself.

Sources of Fluids and Conditions of Sulfide Deposition

Evidence from Fluid Inclusions

Microthermometric measurements were made on primary and secondary fluid inclusions in quartz from quartz-sulfide veins from the stockwork zone of the NSB and in calcite intergrown with sulfides in massive mineralization from the NSB and SSB. Two-phase (aqueous fluid + vapor bubble) primary inclusions have relatively uniform phase ratios, and lack evidence for boiling or phase separation at the site of mineral precipitation. Eutectic and intermediate melting of CaCl_2 and NaCl hydrates, $\text{CaCl}_2 \cdot 2\text{H}_2\text{O}$ (antarticite) and $\text{NaCl} \cdot 2\text{H}_2\text{O}$ (hydrohalite) indicate that the fluids are best modeled in the H_2O -NaCl- CaCl_2 system. The inclusion fluids have an estimated $\text{CaCl}_2/\text{NaCl}$ ratio of about 0.57. Salinities of primary and secondary inclusion fluids, calculated using the temperature of final ice disappearance (between -12.7 and -4.3°C) range from about 6 to 17 equivalent wt percent NaCl (Fig. 19a). Salinities for primary and secondary inclusions are the same, suggesting that, in spite of the secondary nature of inclusions preserved in calcite, they both contain unmodified hydrothermal fluid trapped in primary inclusions that subsequently was redistributed into lower-temperature secondary inclusions in both quartz and calcite, with their salinities conserved.

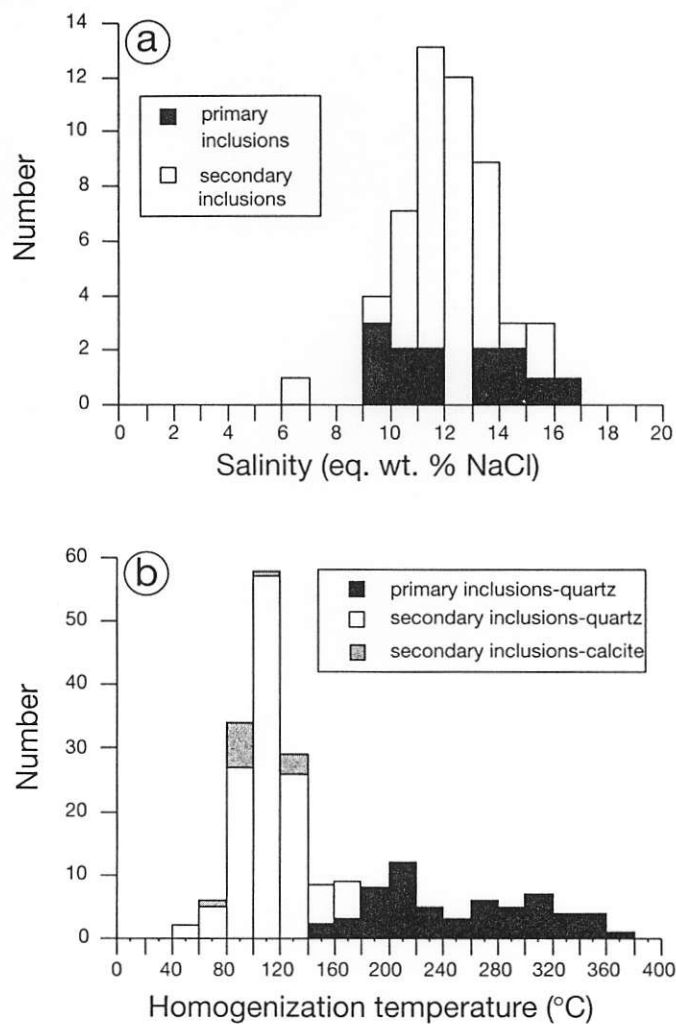


FIG. 19. Frequency histograms of: a. salinities of fluids in primary and secondary, two-phase aqueous inclusions in Windy Craggy stockwork quartz and calcite; b. homogenization temperatures of primary and secondary, two-phase aqueous inclusions in Windy Craggy stockwork quartz and calcite (after Peter and Scott, 1993).

Homogenization temperatures of primary inclusions in quartz range from about 140° to 375°C (Fig. 19b); these temperatures are very similar to the exit temperatures of fluids venting at many modern sea-floor hydrothermal sites (up to about 400°C ; Von Damm, 1990, and references therein). Homogenization temperatures for secondary inclusions in stockwork quartz and in calcite within massive mineralization at Windy Craggy range between about 50° and 170°C . Most of the inclusions in calcite appear primary on a textural basis; however, their homogenization temperatures coincide with those of secondary inclusions in quartz. The paucity of primary, high-temperature inclusions in the massive mineralization may be attributed to the higher degree of structural deformation of the sulfide mass, compared to the underlying stockwork zone that is in more competent, silicified basalts and argillites. The absence of high-temperature inclusions in calcite is attributed to the ready recrystallization of carbonate in response

to metamorphic and/or deformational events. Earlier-formed primary fluid inclusions would have reequilibrated in response to such events, and would thus record lower temperatures (though not lower salinities). The conspicuous absence of any low-salinity fluids in the primary inclusions suggests that such fluids were not present.

It is possible to constrain the water column pressure required to suppress boiling or phase separation by considering the physical and chemical properties of a hot NaCl solution (Bischoff and Pitzer, 1985) in light of the fluid inclusion microthermometric data. For a fluid at a maximum temperature of 375°C and 10 to 15 wt percent NaCl, a confining pressure of about 195 bars is required to suppress phase separation or boiling (Fig. 20). Thus, the Windy Craggy deposit formed under a water column of at least 1,950 m. The pressure correction for a 1,950 m water column overlying the deposit corresponds to about 25°C at a homogenization temperature of 200°C, and about 10°

at 350°C (Potter, 1977); these corrections must be added to the homogenization temperatures to obtain minimum estimates of the true trapping temperature.

In order to explain the large size of Windy Craggy, it is tempting to suggest that the sulfides were precipitated from dense, bottom-hugging fluid; it is reasoned that the former process results in concentration and preservation of metals. For deposition from a bottom-hugging fluid to occur, the fluid of a given temperature must be more dense than ambient seawater. Volumetric properties of the inclusion fluids indicate that the endmember mineralizing hydrothermal fluids at Windy Craggy were less dense than seawater and not bottom-seeking as they vented onto the sea floor. For example, at ~2,000 m water depth (200 bars pressure), a fluid of 17 wt percent NaCl—the most saline primary fluid—must be cooler than about 180°C in order to be more dense than seawater.

As pointed out by Turner and Campbell (1987), fluids at 375°C and 10 to 15 wt percent NaCl would become denser than seawater upon mixing (i.e., the originally buoyant plume would reverse buoyancy). Fluids of salinity greater than ~7 to 8 wt percent NaCl are required to produce reversing buoyancy for a 375°C fluid. The Windy Craggy fluids are more saline than this (Fig. 19a) and would have risen in the water column in a similar manner to that of present-day black smokers on the sea floor and subsequently reversed buoyancy. This would have important implications for the style and efficiency of metal precipitation if these reversed buoyancy fluids collected in a depression on the sea floor. However, the paucity of primary layering within the sulfides suggests that this did not happen at Windy Craggy and indicates that the fluids may have vented from a fault scarp perched above the basin floor. The sulfides were precipitated both in the subsurface within the feeder zone and at the sea floor in sulfide mounds from an (originally) buoyant, black-smoker-like, high-temperature fluid. As the fluids traveled away from the vent site, any sulfides not precipitated at the vent site and entrained in the reversed density plume would have been oxidized.

The Windy Craggy inclusion fluids have salinities that are three to four times greater than that of modern seawater (~3.2 wt percent NaCl; Bischoff and Rosenbauer, 1984). These fluids are much more saline and dense than those measured for many ancient Phanerozoic massive sulfide deposits (e.g., 3.5 to 7.0 equiv wt percent in Kuroko deposits; Pisutha-Arnond and Ohmoto, 1983). They also are more saline than all known fluids venting from the modern sea floor except those in the Red Sea: (e.g., Guaymas basin 3.7 to 8.1 equiv wt percent NaCl; Peter and Scott, 1988; 21°N, EPR 2.9 to 3.8 equiv wt percent NaCl; Le Bel and Oudin, 1982). The cause of the high salinities of the Windy Craggy inclusion fluids is enigmatic; several processes have been proposed to explain the high salinity of such fluids in both ancient and modern hydrothermal systems.

Phase separation or boiling can result in the formation of high salinity fluids (e.g., Butterfield et al., 1990), but adjacent primary fluid inclusions from Windy Craggy do not

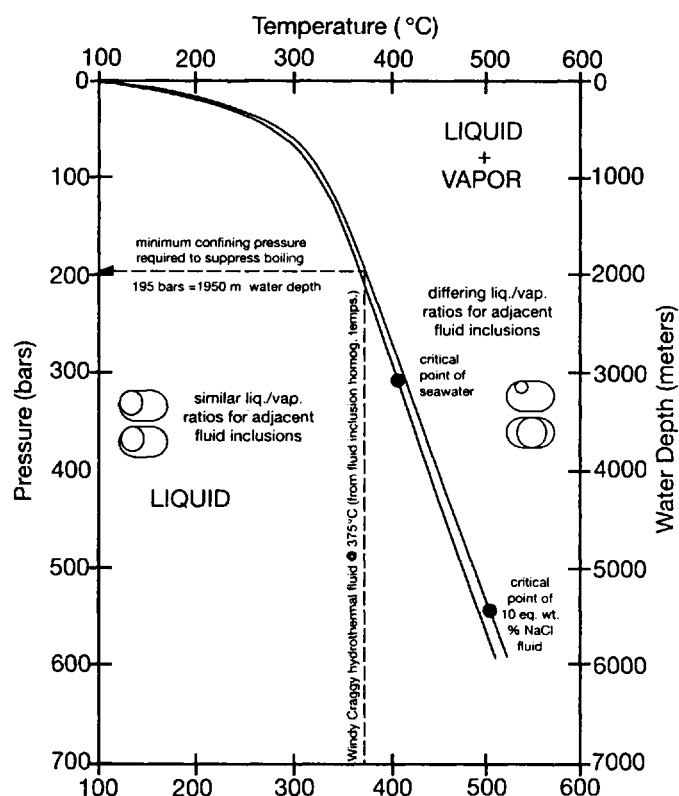


FIG. 20. Temperature-pressure-composition relations for seawater (3.2 wt % NaCl; Bischoff and Rosenbauer, 1984) and a fluid of 10 equiv wt % NaCl salinity (after Roedder and Bodnar, 1980). Shown are the two-phase curve and critical point for each of these fluids. For fluids trapped in inclusions within the one-phase region, adjacent inclusions will display constant liquid-to-vapor ratios. Adjacent fluid inclusions that have trapped a boiling fluid in the two-phase region may contain drastically different phase ratios. Primary Windy Craggy fluid inclusions display constant phase ratios and indicate that the fluids were not boiling at the site of mineral deposition. This allows constraints to be placed on the minimum water depth at which the inclusions formed. From the inclusion data, a representative primary inclusion fluid at 375°C and 10 to 15 equiv wt percent NaCl (salinity has only a minor effect at this temperature) must have been trapped at a minimum pressure of 195 bars in order for boiling to have been suppressed (after Peter and Scott, 1993).

display variable liquid-to-vapor phase ratios that would provide evidence for boiling or phase separation at the site of mineral deposition. Phase separation could have occurred deeper in the subsea floor, but it is not thought to have occurred in the feeder zones as they do not extend below the massive sulfides for great vertical distances. Alternatively, this process may have occurred in the recharge area.

Hydrothermal fluids of the Atlantis II Deep have salinities in the range of 12 to 23 equiv wt percent NaCl (Rambouz et al., 1988), which were attained by leaching of extensive, 2- to 4-km-thick, evaporite beds. Leaching of evaporites to account for elevated salinities at Windy Craggy is not favored here because geologic mapping and diamond drilling have not identified the presence of even minor evaporite beds in the vicinity of the deposit (i.e., in the footwall). Furthermore, the presence of an evaporite component in the fluids would be reflected in the sulfur isotope composition of the precipitated sulfides, but this is not the case at Windy Craggy (see below).

Seyfried et al. (1986) proposed that hydrothermal fluid salinities can become elevated above seawater by the formation of Fe hydroxylchlorides via hydration reactions between hydrothermal fluid and basalts and/or sediments in the subsurface. This possibility can be tested by a simple mass-balance calculation: experimental observations indicate that hydrothermal alteration of basalts at temperatures of about 300°C, and which contain predominantly the minerals quartz and chlorite, formed at water/rock ratios (W/R) of >50 (e.g., Mottl, 1983). Based on the experimental data of Seyfried and Mottl (1982) on Na uptake and leaching from basalts, Peter (1992) estimated the W/R for Windy Craggy to have been >10. A lower limit for the integrated W/R in stockwork domains at Windy Craggy can be calculated by comparing the total mass of altered rock to the mass of fluid necessary to transport the metals contained in the massive sulfides, in a manner similar to that of Lowell and Rona (1985). The very conservative assumptions made in the calculations are: (1) all of the Fe in the deposit was leached from the underlying basalt and argillite; (2) the massive sulfide is composed entirely of pyrite; (3) all of the Fe in solution is precipitated; (4) all of this Fe is precipitated at the sea floor, and Fe present in sulfides disseminated in the stockwork zone beneath the deposit is ignored; and (5) fluids at 300° to 350°C are assumed to carry 100 ppm Fe, as in black smokers on the East Pacific Rise (Von Damm, 1990) and in the lower brine of the Atlantis II Deep, (Brooks et al., 1969), although there is considerable variation in the Fe contents of modern hydrothermal vent fluids (e.g., Von Damm, 1990).

Massive sulfide reserves at Windy Craggy are about 300 Mt (300×10^9 kg) FeS_2 , corresponding to 100×10^9 kg of Fe. Applying the foregoing assumptions, the mass of hydrothermal fluid that would have vented at the sea floor is 1×10^{15} kg. From underground mapping and drill core information, the dimensions of visibly altered footwall rocks was measured and, to allow for possible alteration evident only on a microscopic scale, these dimensions are

increased by a generous factor of 10 to give an estimated mass of 0.9×10^{12} kg of hydrothermally altered rocks. At a density of 2.70 gm/cc for unaltered rock (basalt ~2.73 and calcareous shale ~2.67), a minimum W/R of ~580 by weight is indicated. Clearly, salinities of the hydrothermal fluids could not have been significantly modified under such highly water-dominated conditions; the high salinities of the fluids must have resulted from some other process.

The last possibility to explain the high salinities is the presence of a saline magmatic fluid component (e.g., Urabe and Marumo, 1991) in the inclusions. Hot, highly saline fluids are characteristic of the high-temperature stages of porphyry copper mineralization where concentrated solutions may result from the condensation of supercritical magmatic fluids into a liquid phase containing the bulk of the solute (e.g., Roedder, 1981). Such dense magmatic fluids could have mixed effectively with solutions in a subsea-floor convection system under hydrostatic conditions. Proof for this hypothesis, however, is elusive (e.g., see de Ronde, 1995). As pointed out by Shanks et al. (1995), the low water content of sea-floor basaltic rocks, together with the lack of magma saturation with respect to water at eruption depths of more than a few hundred metres, indicates that such lavas do not exsolve water at depths greater than a few hundred meters simply by quenching to form a glass. Rather, complete crystallization of a large mafic intrusion to only anhydrous phases would be required to release substantial amounts of magmatic water. There are no sufficiently large intrusions known beneath Windy Craggy that might have served as the possible source for magmatic fluids, and currently there is no isotopic or other evidence to suggest the presence of such fluids.

Evidence from Sulfur Isotopes

Sulfur isotope ratios of sulfide minerals from the NSB stockwork, and of massive sulfide from both zones, can be used to constrain the source(s) of sulfur and, by inference, metals in the deposit. Fractionation of sulfur isotopes between coexisting sulfide pairs may be used to estimate temperatures of sulfide precipitation or subsequent recrystallization. Most $\delta^{34}\text{S}$ values for Windy Craggy sulfides cluster between -0.5 and 3.0 per mil (mean = 0.9 ± 1.8 (1 σ); n = 36) (Fig. 21).

The two principal sources of sulfur for the deposit are the host rocks (basalt and argillite) and seawater. Unaltered Windy Craggy basalts and sills contain ~500 ppm sulfur, and the argillite host rocks typically have 1,000 to 5,000 ppm (Peter, 1992). Some or all of this sulfur in the Windy Craggy rocks might have been mobilized during interaction with heated seawater or other hydrothermal fluids. Leaching of basaltic sulfur by hydrothermal fluids has been demonstrated experimentally (Mottl et al., 1979). Interaction of hydrothermal fluids with underlying basalts at Windy Craggy is indicated by Pb isotope studies of sulfides and basaltic and argillaceous host rocks (Peter, 1992). However, $\delta^{34}\text{S}$ values of sulfides at Windy Craggy are slightly more positive than those of basaltic sulfur (0.1

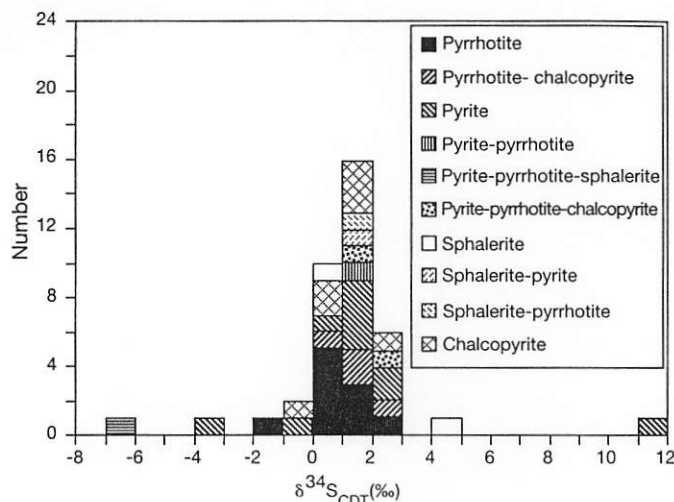


FIG. 21. Frequency histogram of $\delta^{34}\text{S}$ values of Windy Craggy sulfide samples (after Peter and Scott, 1993). One outlier, a sample of coarse cubes of diagenetic pyrite in argillite from about 170 m stratigraphically below and along strike from the SSB (i.e., likely unrelated to hydrothermal activity and alteration), has a $\delta^{34}\text{S}$ value of -3.1‰ that may be representative of the argillites. A sample of colloform pyrite from a pyrite-calcite vein genetically unrelated to the deposit, and about 1,100 m stratigraphically below the sulfide mass and about 700 m below the lowermost part of the feeder zone, has a $\delta^{34}\text{S}$ value of 11.1‰ . Two analyses of pyrite from the East Arm prospect, a massive sulfide occurrence about 7 km east of Windy Craggy in lithologically, geochemically, and temporally similar rocks, have $\delta^{34}\text{S}$ values of 1.7 and 2.4‰, which are very similar to those for sulfides from Windy Craggy.

$\pm 0.5\text{‰}$; Sakai et al., 1984) and require an additional source of isotopically heavy (^{34}S) sulfur. The most likely source of this ^{34}S -enrichment is seawater sulfate.

The sulfur isotope composition of Upper Triassic seawater was about 15 to 16 per mil (Claypool et al., 1980). Ferrous iron in basalt (and sedimentary rocks) has the capacity to reduce seawater sulfate, provided the temperature of interaction exceeds about 300°C (e.g., Shanks et al., 1981). Iron in the hydrothermal fluid is also an effective reducing agent. If seawater sulfate was the sole source of sulfur for Windy Craggy sulfides, fractionation factors require temperatures ranging from 370° to 380°C for the hydrothermal fluids (Shanks et al., 1981). However, according to Mottl et al. (1979), complete reduction of seawater sulfate is limited to settings in which the W/R ratio is ≤ 6 , due to the limited supply of Fe^{2+} in basalts. At Windy Craggy, W/R ratios were ≥ 50 . Sulfate reduction is further limited by the requirement that some Fe^{2+} be available for the formation of chlorite, which is the only common ferromagnesian aluminosilicate phase to form at temperatures $>300^\circ\text{C}$ in submarine hydrothermal systems. Therefore, inorganically reduced seawater sulfate could only have been a minor contributor of sulfur, compared to that derived from the basaltic host rocks. $\delta^{34}\text{S}$ values of sulfides in many modern sea-floor hydrothermal sites on unsedimented ridges are similar to those measured for Windy Craggy sulfides (1–7‰; see compilation in Shanks et al., 1995). Only a small component of reduced seawater sulfate (25–33% of the total sulfide) is necessary to account

for the range of sulfur isotope compositions in submarine sulfides from unsedimented ridges (Shanks et al., 1995).

Mass-balance calculations imply that the contribution of Triassic marine sulfate was about 10 to 15 percent of the total sulfur in the Windy Craggy mineralizing fluids. Several sulfide samples have isotopically light (negative $\delta^{34}\text{S}$) compositions, reflecting the input of bacterially-reduced sulfur. Bacterially mediated sulfate reduction in pore waters or reducing marine sediments is well established (e.g., Goldhaber and Kaplan, 1975) and produces iron sulfides with sulfur isotope compositions variably more negative by 15 to 45 per mil than the initial seawater sulfate. Bacterially reduced sulfur derived from sedimentary rocks was not volumetrically important in formation of the Windy Craggy deposit because only a few of the analyzed samples are depleted in ^{34}S .

Evidence from Carbon and Oxygen Isotopes

Oxygen and carbon isotope data were obtained for calcite and siderite that are ubiquitous within the massive mineralization. The $\delta^{13}\text{C}$ values of calcites range from -4.1 to $+6.0$ per mil (median = -0.3 ; $n = 31$), and $\delta^{18}\text{O}$ (calcite) varies from 10.9 to 20.7 per mil (median = 12.9‰ ; $n = 31$). The $\delta^{13}\text{C}$ and $\delta^{18}\text{O}$ values of siderite range from -8.8 to 1.1 per mil (median = -1.5 ; $n = 10$) and 7.6 to 23.3 per mil (median = 13.1‰ ; $n = 10$), respectively. There are several possible sources for the carbon in the Windy Craggy carbonates: magmatic, seawater, diagenetic degradation of organic matter in the argillaceous sediments, dissolution of primary marine carbonate (e.g., biogenic material, ooids, or pelagic precipitates), oxidation of methane, or combinations of these sources and processes. These sources may be distinguished isotopically. Modern seawater and primary marine carbonates have $\delta^{13}\text{C}$ values near 0 per mil. The lowest $\delta^{13}\text{C}$ value observed for carbonate in modern oxygen-deficient marine water is about -7 per mil, for samples from a depth of 1,500 m in the Black Sea (Deuser, 1970). Oxygen isotope compositions of marine carbonates exhibit a $\delta^{18}\text{O}$ range from ~ -0.8 to ~ 2.0 per mil (Sheppard, 1986). Carbon and oxygen isotope compositions of sedimentary carbonates at Windy Craggy were not measured; however, values for Triassic marine carbonates range from about -11 to 4 per mil for $\delta^{13}\text{C}$ and between 15 and 36 per mil for $\delta^{18}\text{O}$ with most $\delta^{18}\text{O}$ values falling between 24 and 31 per mil (Veizer and Hoefs, 1976). The $\delta^{18}\text{O}$ value of Triassic seawater is estimated to have ranged between -5 and 0 per mil (Karhu and Epstein, 1986).

Organically derived carbon has $\delta^{13}\text{C}$ values as low as -20 to -30 per mil (e.g., Berger and Vincent, 1986). Anaerobic methane oxidation also produces similar negative $\delta^{13}\text{C}$ values (Devol et al., 1984). This process, in addition to forming ^{13}C -depleted methane, would produce ^{13}C -enriched carbonate cements (Hudson, 1977). Dilution of purely organic-derived bicarbonate by marine bicarbonate may occur in pore waters to yield intermediate values of $\delta^{13}\text{C}$ (Coleman et al., 1982). Coleman and Raiswell (1981) provided an example of this in which CO_2 formed by bacterial sulfate reduction is mixed with dissolved bicarbonate to produce carbonate minerals having $\delta^{13}\text{C}$ values of about -15 per mil.

Measured $\delta^{13}\text{C}$ values of calcite and siderite from Windy Craggy range from -8.8 to 6 per mil and cluster around -5 to 3 per mil. These data suggest that the predominant source of carbon was dissolved marine carbonate. Most of the Windy Craggy carbonate $\delta^{13}\text{C}$ values are distinctly heavier than those observed for deep-seated or mantle-derived carbon, which have $\delta^{13}\text{C}$ between -4.1 and -3.4 per mil (Gerlach and Taylor, 1990). On this basis, a significant contribution of magmatic carbon is ruled out.

Fluid $\delta^{13}\text{C}$ values based on temperatures estimated from other isotopic data (Peter, 1992) and fluid inclusions range from -2.7 to 6.9 per mil and $\delta^{18}\text{O}$ values from -0.7 to 14.4 per mil. The lower parts of these ranges of isotopic compositions are reasonable for bottom waters at the vein site, which probably consisted of a mixture of Triassic seawater with $\delta^{18}\text{O}$ values between -5 and 0 per mil (Karhu and Epstein, 1986), and a large component of ^{18}O -enriched hydrothermal fluid generated from this bottom seawater that convected through Triassic volcano-sedimentary strata having $\delta^{18}\text{O}$ values of 15 to 36 per mil.

The isotopic compositions of Windy Craggy fluids are more ^{18}O -enriched than the fluids sampled to date from modern hydrothermal black smokers (-0.2 – 2.1 ‰; see summary in Shanks et al., 1995) and from brines in the Red Sea (1 – 2 ‰; Craig, 1969). The origin of such extremely ^{18}O -enriched ore-forming solutions in volcano-genic massive sulfide deposits remains controversial (e.g., Beatty et al., 1988) and several possible mechanisms have proposed: (1) participation of juvenile, magmatic or metamorphic fluids in addition to seawater (e.g., Urabe and Marumo, 1991); (2) expulsion of isotopically evolved connate fluids of marine origin (Pisutha-Armond and Ohmoto, 1983); (3) high-temperature interaction of seawater with rocks under low W/R conditions (e.g., Bowers and Taylor, 1985); (4) exchange with ^{18}O -enriched volcanic or sedimentary rocks (Barriga and Kerrich, 1984); (5) multi-pass convection; (6) enrichment by shale ultra-filtration which involves water circulating through shale or clay units and undergoing extensive fractionation that causes the residual water to be enriched in $\delta^{18}\text{O}$ over the starting water and ultra-filtrate (Coplen and Hanshaw, 1973); or (7) prior evaporation of seawater in a closed basin (Craig and Gordon, 1965).

The most geologically reasonable of these possibilities for Windy Craggy is the interaction of hydrothermal fluid with ^{18}O -enriched footwall sedimentary rocks. Detrital sedimentary rocks generally are relatively enriched in $\delta^{18}\text{O}$ (Taylor, 1980). Most clay minerals have $\delta^{18}\text{O}$ values between 15 and 30 per mil (e.g., Savin and Epstein, 1970a), and those of oceanic sediments range between 9 and 13 per mil on a carbonate-free basis (Savin and Epstein, 1970b). Formation waters are typically enriched in ^{18}O from exchange with subsurface sediments (e.g., Kharaka et al., 1973). Thus, interaction of hydrothermal fluids with the footwall argillites under moderate W/R conditions and elevated temperatures could have increased the $\delta^{18}\text{O}$ of the fluids.

The $\delta^{13}\text{C}$ values of the carbonates are inconsistent with a magmatic source for the carbon; however, oxygen isotope data for argillite host rocks at Windy Craggy are

needed to eliminate this possibility. Seawater in arid regions is enriched in D and ^{18}O due to evaporation, and this could explain the high salinities of the Windy Craggy fluids. Evaporative processes to explain the high salinities and ^{18}O -enriched nature of the fluids at Windy Craggy are not favored, given the water depths implied from the fluid inclusion data. Such closed-system processes also require a restricted body of water that also would appreciably affect the carbon isotopic composition of the hydrothermal fluids and precipitated carbonates (i.e., both would become enriched in ^{13}C ; Stiller et al., 1985), but the carbon isotope compositions of Windy Craggy carbonates are not readily explained by such processes. Furthermore, the faunal populations at Windy Craggy would not tolerate major changes in salinity.

Evidence from Lead Isotopes

Figure 17 is a $^{207}\text{Pb}/^{204}\text{Pb}$ vs. $^{206}\text{Pb}/^{204}\text{Pb}$ plot for Windy Craggy bulk sulfides, basalt, and argillite. The data for massive sulfide only define a linear array of limited extent (line "A") that is interpreted to reflect mixing of Pb from a mantle source (the footwall basalts) with that from an upper crustal source (the terrigenous sediments intercalated with the footwall basalts, or an unidentified source). The Pb isotope composition of Windy Craggy sulfides is intermediate between those of MORB and pelagic sediment, supporting a genetic model that involves mixing of Pb from oceanic tholeiites and sediments.

The Pb isotope data for volcanic and sedimentary host rocks of the deposit also define a linear trend but with a shallower slope (line "B"; Fig. 17) that represents radiogenic growth of Pb since the time of deposition. The least radiogenic composition of this trend intersects an intermediate composition on the sulfide trend, and this point of intersection is interpreted to be the initial Pb isotope composition of the host rocks at the time of mineralization.

Similarity in the initial Pb isotope compositions of the volcanic and sedimentary host rocks at Windy Craggy reflects either derivation of the sedimentary rocks from the proximal volcanic rocks and inheritance of their Pb isotope compositions, or homogenization of the Pb isotope compositions of the host rocks by hydrothermal convection of fluids. Correspondence of the bulk geochemical signatures for the host igneous and sedimentary rocks supports the former interpretation.

Hydrothermal Alteration

Footwall host rocks of the Windy Craggy deposit are hydrothermally altered to chlorite and quartz; evaluation of the potential alteration of hanging wall host rocks was not done due to the lack of exposure (and drillcore) of these rocks. Chloritized basalts contain predominantly massive, interlocking, fine-grained, felted, pleochroic, medium green chlorite (60–95%) that displays Berlin blue birefringence. Also present are very fine-grained sphene, subhedral disseminated epidote (0–7%), abundant calcite (5–10%), and quartz (2–5%) as ragged patches, and disseminated, fine-grained euhedral ilmenite (trace to 1%). Minor sulfides comprise fine-grained euhedral cubes of

respectively. For the chloritized basalts, the elements Al, P, Zr, Ta, Lu, and Yb were the least mobile and these define an isocon equivalent to constant mass or a 7.6 vol percent loss for this sample (Fig. 22a). For the silicified basalts, Al, Tb, Yb, Lu, Zr, and Sm were the least mobile, together defining an isocon equivalent to a 346 vol. percent gain for this sample (Fig. 22b).

Overall, for chloritized basalts volume changes vary from a 7.6 percent loss to a 52 percent gain, although most samples lack evidence for volume change (i.e., isovolumetric). Silicified basalts show significant volume gains from 216 percent to 1,031 percent, with most samples displaying gains of 350 to 500 percent. Figures 22a, b also show losses and gains for elements and components. Chloritized basalts display large additions of Fe_2O_3 , Au, Co, and U, large depletions of Na, K, Rb, Ca and smaller depletions of Mg; LREE and MREE (La, Ce, Nd, Sm, Eu and Tb) show very slight gains or losses (Figs. 22a, 23a). Silicified basalts display major additions of S, Si, U, and

Au, lesser additions of Mn and P, and depletions of Na, Ba, Sr, Mg, Ni, Co, and Cr. The LREE and MREE have been slightly to significantly depleted, with the exception of several small Eu gains (Figs. 22b, 23b).

Although chloritization of Windy Craggy basalt was in places an isovolumetric process, silicification of basalt was accompanied by large gains in volume. Such gains in the former were manifested, at least in part, by intense brecciation during silicification. The strong addition of Fe and concomitant loss of Mg in chloritized basalt reflects the destruction of primary Mg-bearing minerals and the formation of Fe-rich chlorite. In silicified basalt and argillite, the addition of Fe records the introduction of finely disseminated Fe-bearing sulfides.

End-member hydrothermal vent fluids (i.e., no entrained ambient intermixed seawater) associated with modern seafloor sulfide deposits are characterized by a conspicuous absence of Mg (e.g., Von Damm, 1990). Depletion of Mg in the Windy Craggy stockwork indicates that this upflow zone probably formed from fluids similarly depleted in Mg. It can be deduced from the above mass balance calculations that silica and iron were present in the hydrothermal fluid, and were added to the volcanic and sedimentary rocks during alteration. This is in agreement with experimental studies of the alteration of organic-rich sediment, graywackes, and basalt by hot seawater (e.g., Thornton and Seyfried, 1987; Berndt et al., 1989).

Experimental studies indicate that quartz solubility in water is strongly dependent on temperature (e.g., Fournier, 1985). Only at temperatures $<350^\circ\text{C}$, and at higher temperatures where pressure is >900 bars, does quartz solubility decrease markedly with decreasing temperature. Silicification, therefore, probably resulted from the cooling of hydrothermal fluids that were initially $<350^\circ\text{C}$.

Experimental studies indicate that K mobility is mainly a function of temperature ($>150^\circ\text{C}$; Menzies and Seyfried, 1979); K is less soluble at lower temperatures (Seyfried and Bischoff, 1979). Sodium mobility, however, is dependent primarily on the effective water/rock ratio (W/R). The effective W/R ratio depends on the history of the water (e.g., convective circulation). Circulation of water through rocks causes the effective W/R ratio for a unit mass of water to decrease and the effective W/R ratio for a unit mass of rock to increase, even if the true W/R ratio remains constant. At W/R ratios >10 , Na is leached from basalt and enriched in solution (Seyfried and Bischoff, 1977), whereas at W/R ratios ≤ 5 Na is removed from seawater and fixed in basalt (e.g., Mottl and Holland, 1978). In light of these experimental data, Windy Craggy mineralizing fluids are interpreted to have had temperatures of $>150^\circ\text{C}$ and W/R ratios of >10 .

Chloritized basalts from Windy Craggy exhibit slightly positive Ce additions, relative to adjacent REE, which is indicative of reducing conditions. In contrast, the most intensely silicified basalts display Ce depletions, relative to adjacent REE, which is indicative of conditions that were more oxidizing than those within the chloritized basalts (cf. Sverjensky, 1984).

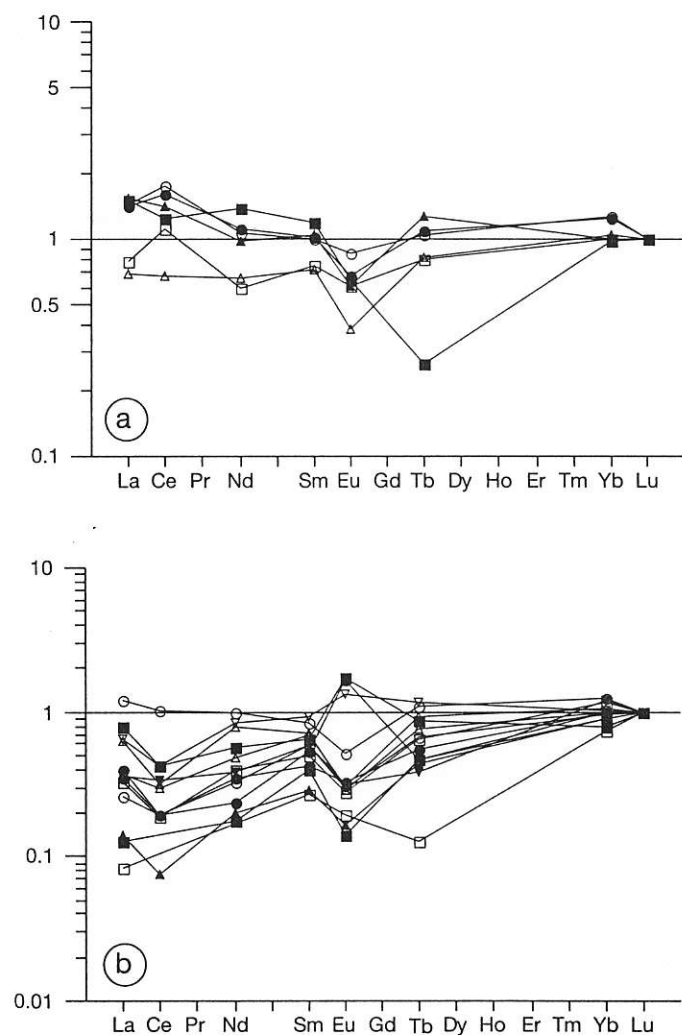


FIG. 23. Rare earth element plots of: a. Windy Craggy chloritized basalt normalized to average, least-altered basalt and doubly-normalized to Lu; b. silicified Windy Craggy basalt-normalized to average, least-altered basalt and doubly-normalized to Lu.

Conclusions

The Windy Craggy Cu-Co-Au deposit in the northern Canadian Cordillera is the world's largest of the (>300 Mt) Besshi-type, averaging about 1.5 wt percent Cu and 0.08 wt percent Co with local Au-rich zones. It lies within the informally named Tats Volcanic Complex, an Upper Triassic volcano-sedimentary sequence in northwestern British Columbia. The deposit consists of two major massive sulfide lenses, each with an underlying stockwork zone that cut Upper Triassic lower greenschist facies basalt flows and argillites. On a broad scale, the massive sulfides occur at or near the transition from the sedimentary to the overlying volcanic rocks. Footwall rocks immediately underlying the sulfide bodies are predominantly chloritic pillowed basalts containing quartz-sulfide stringer veins and disseminated sulfides.

Intercalated basalt flows and sills and turbiditic argillite in the Windy Craggy area were deposited in a marine setting, as evidenced by occurrence of well-developed pillows, turbidites (fine- to very fine grained, D-E facies), marine macro- and microfossils. Furthermore, the fossils indicate an open marine setting of normal seawater salinity. Although deep-water conditions are thought to have prevailed, there are no diagnostic water depth indicators. Mafic magma was intruded into the sediments as sills and extruded as flows in a tectonically active basin in which turbiditic sedimentation was taking place. The flows and sills are LREE-enriched and have minor and trace element abundances characteristic of tholeiitic and transitional to subalkaline basalts.

Massive sulfides consist mainly of pyrrhotite, pyrite, and chalcopyrite with minor amounts of chalcocite, marcasite, digenite, and sphalerite, and rare gold, electrum, marcasite, and arsenopyrite; gangue minerals are predominantly quartz, chlorite, magnetite, calcite, siderite, and stibnomelane, with minor ankerite and hisingerite. The abundance of massive, fine-grained to recrystallized textures and presence of locally abundant breccia clast textures in the massive sulfides and the relative paucity of laminated sulfides indicate that the sulfides accumulated at the sea floor by chimney and mound formation. Sulfides have been annealed, recrystallized, and remobilized, both on the sea floor and during subsequent deformation and metamorphism. Breccia textures within the sulfide mass indicate that mound and chimney erosion were important locally. The presence of minor bedded to laminated sulfides in argillite at the footwall contact of the SSB, and ferruginous cherts also suggest that some sulfides and oxides precipitated on the sea floor as fallout from a hydrothermal plume in the ambient water column. Replacement textures within footwall argillite and stockwork veins indicate that these sulfides were precipitated in the subsurface. Post-depositional deformation processes resulted in some transposition of the sulfide lenses from their underlying feeder zones.

Both chloritized and silicified hydrothermal alteration facies are recognized. Argillite was not heavily chloritized relative to basalt. Chloritization of the basalt was approximately isovolumetric, whereas silicification was characterized by

significant volume increases. During silicification of the basalts, LREE and MREE were significantly mobilized, but during chloritization there was only limited REE mobility. The silicified zone is interpreted to have formed when the W/R ratio increased, and the preexisting chlorite alteration assemblage in the volcanics and the sedimentary rocks was overprinted (by conductive cooling and mixing of the hydrothermal fluid with seawater) in the fractured conduit).

Fluid inclusion microthermometry indicates that the hydrothermal fluids from which the massive sulfides precipitated were at minimum temperatures of ~220° to 380°C, similar to vent fluids from many modern sea-floor sulfide deposits, and did not undergo phase separation at the site of mineral deposition. Salinities of the fluids range from 9 to 17 equiv wt percent NaCl, with a mean of about 12 equiv wt percent NaCl. The process by which the salinity of this fluid was enhanced has not been identified. At these temperatures and salinities, the vent proximal fluids were less dense than seawater, similar to present-day black smokers on the sea floor, and sulfide precipitation commenced in the subsurface within the feeder zone and also occurred at the seafloor in sulfide mounds. On mixing with seawater, these fluids cooled and reversed buoyancy, and as they traveled away from the vent site, any sulfides which subsequently were precipitated, or that were entrained in the reversed density plume, were oxidized. Based on the absence of evidence for phase separation, water depths must have been at least 1,950 m.

Sulfur isotope compositions of sulfides indicate that sulfur in the deposit was leached primarily from the host basalts, with a minor component derived from inorganically-reduced seawater sulfate. For all but three samples, there is no evidence for the incorporation of bacterially derived sulfur. Carbon isotope analyses suggest that dissolved marine carbonate or seawater was the predominant source of carbon in the carbonate minerals. Calculated carbon and oxygen isotope compositions are consistent with the Windy Craggy hydrothermal fluid having been seawater that became enriched in ¹⁸O upon reaction with sedimentary host rocks in the subsurface during hydrothermal circulation. The Pb isotope geochemistry of the sulfides indicates that the Pb was derived from the host basalts and argillites. The Pb isotope compositions of the host basalt and argillite indicate that they had similar initial Pb isotope ratios. These data suggest that the argillite is compositionally immature and was derived mainly from the basalts, or that the Pb isotope compositions of all the host rocks were homogenized by the hydrothermal alteration that accompanied sulfide deposition.

Windy Craggy exhalites are similar in their Fe and Mn abundances to other ferruginous cherts associated with massive sulfide deposits and to modern metalliferous sediments. The REE signatures of the Windy Craggy exhalites vary from being like those of modern hydrothermal vent fluids, to like those of modern seawater. Positive Eu anomalies, typical of modern hydrothermal fluids, correlate positively with Fe and Mn contents, and both are related to hydrothermal activity.

The trace and REE geochemistry of argillites intercalated with the basaltic rocks suggests that these sediments were not eroded from a continental land mass, but rather were derived locally from basalts similar in composition to those of the Windy Craggy area. Major element geochemistry shows a significant hydrothermal contribution of Fe and Mn in the argillites. Distinctive negative Ce anomalies in the REE patterns of the argillites are inherited from seawater.

Geological evidence, tectonic discrimination using the trace element geochemistry of the argillites, the trace element and REE geochemical signatures of the intercalated basalt sills and flows, and the lead isotope ratios of the host basalts, argillites and sulfides indicate the Windy Craggy deposit likely formed in a rifted, mature, oceanic, back-arc basin setting. The trace and minor element abundance patterns of the Windy Craggy basalt flows and sills are similar to those found in some back-arc basin basalts. Dikes that cut all other rock types, including mineralized rocks, display characteristic depletions of Ta and Nb that reflect the influence of a subducting slab in an arc environment. However, this arc rifting occurred much later, (no ages are available) after the Windy Craggy massive sulfides and host rocks were deposited, and is unrelated to formation of the deposit.

Modern Besshi-type deposits (e.g., Middle Valley and Juan de Fuca Ridge, Mottl et al., 1994; Escanaba trough, Zierenberg et al., 1993) are forming near continental land masses, and their host clastic sediments are continentally derived. The Windy Craggy deposit is, however, not similar in these regards. The giant size of the Windy Craggy deposit is as yet unexplained, but the excellent preservation of primary features and low metamorphic grade makes this the best-preserved example of an ancient Besshi-type massive sulfide deposit in the world.

Acknowledgments

We thank Douglas Little, Gerald Harper, Bruce Downing, Nicholas Callan, Mary Webster, Geddes Webster, and Robert Beckett, all formerly of Geddes Resources Ltd., for support, assistance, discussions, and friendship. Research funding came from NSERC Operating and Strategic grants, a Bank of Nova Scotia grant to the Marine Geology Research Laboratory, a British Columbia Ministry of Energy, Mines, and Petroleum Resources research contract, a Geological Society of America Research Grant, an H.V. Ellsworth Fellowship, and Ontario Graduate Scholarships. A.D. Smith kindly provided an unpublished manuscript with geochemical and isotopic analyses of Lower Tatt basalts. We thank Don MacIntyre for discussions on the geology of the Alexander terrane and the Windy Craggy area and Matthew Leybourne for discussions on igneous geochemistry and radiogenic isotopes. Peter gratefully acknowledges the GSC for support in the preparation of this manuscript. This contribution has benefited from reviews by Wayne Goodfellow, John Slack, and Tucker Barrie. This is GSC contribution no. 1997055.

REFERENCES

ddy, S.K., 1979, Rare earth patterns in manganese nodules and micronodules from the northwest Atlantic: *Geochimica et Cosmochimica Acta*, v. 43, p. 1105-1115.

- Ager, F.G., 1965, Mesozoic and Cenozoic Rhynchonellacea; in *Treatise on invertebrate paleontology: Geological Society of America and University of Kansas Press*, p. 604-605.
- Ahern, J.L., and Turcotte, D.L., 1979, Magma migration beneath an ocean ridge: *Earth and Planetary Science Letters*, v. 45, p. 115-122.
- Aumento, F., 1968, The Mid-Atlantic Ridge near 45° N. II. Basalts from the area of Confederation Peak: *Canadian Journal of Earth Sciences*, v. 5, p. 1-21.
- Baker, B.H., Goles, G.G., Leeman, W.P., and Lindstrom, M.M., 1977, Geochemistry and petrogenesis of basalt-benmoreite-trachyte suite from the southern part of the Gregory Rift, Kenya: *Contributions to Mineralogy and Petrology* v. 64, p. 303-332.
- Bamba, T., and Motoyoshi, Y., 1985, Study on massive sulfide ores from the Shimokawa mine, Hokkaido, Japan: *Mining Geology*, v. 35, p. 211-225.
- Barrett, T., Jarvis, I., and Jarvis, K.E., 1990, Rare earth element geochemistry of massive sulfides-sulfates and gossans on the Southern Explorer Ridge: *Geology*, v. 18, p. 583-586.
- Barriga, F.J.A.S., and Kerrich, R., 1984, Extreme ¹⁸O-enriched volcanics and ¹⁸O-evolved marine water, Aljustrel, Iberian pyrite belt: Transition from high to low Rayleigh number convective regimes: *Geochimica et Cosmochimica Acta*, v. 48, p. 1021-1031.
- Batiza, R., and Vanko, D.A., 1985, Petrologic evolution of large failed rifts in the eastern Pacific: Petrology of volcanic and plutonic rocks from the Mathematician Ridge area and the Guadalupe Trough: *Journal of Petrology*, v. 26, p. 564-602.
- Beatty, D.W., Taylor, H.P., Jr., and Coad, P.R., 1988, An oxygen isotope study of the Kidd Creek, Ontario, volcanogenic massive sulfide deposit: Evidence for a high ¹⁸O ore fluid: *Economic Geology*, v. 83, p. 1-17.
- Berger, W.H., and Vincent, E., 1986, Deep-sea carbonates: Reading the carbon-isotope signal: *Geologische Rundschau*, v. 75, p. 249-269.
- Berndt, M.E., Seyfried, W.E., Jr., and Janecky, D.R., 1989, Plagioclase and epidote buffering of cation ratios in mid-ocean ridge hydrothermal fluids: Experimental results in and near the supercritical region: *Geochimica et Cosmochimica Acta*, v. 53, p. 2283-2300.
- Bhatia, M.R., and Crook, K.A.W., 1986, Trace element characteristics of graywackes and tectonic setting discrimination of sedimentary basins: *Contributions to Mineralogy and Petrology*, v. 92, p. 181-193.
- Bischoff, J.L., and Pitzer, K.S., 1985, Phase relations and adiabats in boiling seafloor geothermal systems: *Earth and Planetary Science Letters*, v. 75, p. 327-338.
- Bischoff, J.L., and Rosenbauer, R.J., 1984, The critical point and two-phase boundary of seawater, 200°-500°C: *Earth and Planetary Science Letters*, v. 68, p. 172-180.
- 1985, An empirical equation of state for hydrothermal seawater (3.2 percent NaCl): *American Journal of Science*, v. 285, p. 725-763.
- Bonatti, E., and Joensuu, O., 1966, Deep-sea iron deposit from the South Pacific: *Science*, v. 154, p. 643-645.
- Bonatti, E., Kolla, V., Moore, W.S., and Stern, C., 1979, Metallogenesis in marginal basins: Fe-rich basal deposits from the Philippine Sea: *Marine Geology*, v. 32, p. 21-37.
- Boström, K.B., 1970, Submarine volcanism as a source for iron: *Earth and Planetary Science Letters*, v. 9, p. 348-354.
- Boström, K., 1973, The origin and fate of ferromanganoan active ridge sediments: *Stockholm Contributions in Geology*, v. 27, p. 147-243.
- 1980, The origin of ferromanganoan active ridge sediments, in Rona, P.A., and Lowell, R.P., eds., *Seafloor spreading centers: Hydrothermal systems*: Stroudsburg, Dowden, Hutchinson and Ross, Inc., p. 288-332.
- 1983, Genesis of ferromanganese deposits—diagnostic criteria for recent and old deposits, in Rona, P.A., Boström, K., Laubier, L., and Smith, K.L., Jr., eds., *Hydrothermal processes at seafloor spreading centers*: New York, Plenum Press, p. 473-489.
- Boström, K., and Peterson, M.N.A., 1969, The origin of aluminum-poor ferromanganoan sediments in areas of high heat flow on the East Pacific Rise: *Marine Geology*, v. 7, p. 427-447.
- Bouma, A.H., 1962, Sedimentology of some llysch deposits: A graphic approach to facies interpretations: Amsterdam, Elsevier, 168 p.
- Bowers, T.S., and Taylor, H.P., Jr., 1985, An integrated chemical and stable-isotope model of the origin of midocean ridge hot spring systems: *Journal of Geophysical Research*, v. 90, p. 12583-12606.

- Brooks, R.R., Kaplan, I.R., and Peterson, M.N.A., 1969, Trace element composition of Red Sea geothermal brine and interstitial waters, in Degens, E.T., and Ross, D.A., eds., *Hot brines and recent heavy metal deposits of the Red Sea*: New York, Springer-Verlag, p. 180-203.
- Buchan, R., 1983, Mineralogical Examination of 20 DDH Core Samples from Hole 14-83, Windy Craggy, B.C.: Falconbridge Metallurgical Laboratories, unpublished report MR-1282.
- Butterfield, D.A., Massoth, G.J., McDuff, R.E., Lupton, J.E., and Lilley, M.D., 1990, Geochemistry of hydrothermal fluids from Axial Seamount hydrothermal emissions study vent field, Juan de Fuca Ridge: Sub-seafloor boiling and subsequent fluid-rock interaction: *Journal of Geophysical Research*, v. 95, p. 12895-12921.
- Campbell, R.B., and Dodds, C.J., 1983, Geology of Tatshenshini River Map Area (114P), British Columbia: Geological Survey of Canada Open File 926.
- Cas, R.A.F., and Wright, J.V., 1988, Volcanic successions, modern and ancient: A geological approach to processes, products and successions: London, Unwin-Hyman, 528 p.
- Chaudhuri, S., and Cullers, R.L., 1979, The distribution of rare earth elements in deeply buried Gulf Coast sediments: *Chemical Geology*, v. 24, p. 327-328.
- Chen, C.-Y., and Frey, F.A., 1983, Origin of Hawaiian tholeiite and alkalic basalt: *Nature*, v. 302, p. 785-789.
- Claypool, G.E., Holser, W.T., Kaplan, I.R., Sakai, H., and Zak, I., 1980, The age curves of sulfur and oxygen isotopes in marine sulfate and their mutual interpretation: *Chemical Geology*, v. 28, p. 199-260.
- Coleman, M.L., and Raiswell, R., 1981, Carbon, oxygen, and sulphur isotope variations in concretions from the Upper Lias of N.E. England: *Geochimica et Cosmochimica Acta*, v. 45, p. 133-149.
- Coleman, M.L., Fleet, A., and Donson, P., 1982, Preliminary studies of manganese-rich carbonate nodules from Leg 68, Site 503, Eastern equatorial Pacific: Initial Reports of the Deep Sea Drilling Project, v. 68, p. 481-489.
- Constantinou, G., and Govett, G.J.S., 1973, Geology, geochemistry and genesis of Cyprus sulfide deposits: *Economic Geology*, v. 68, p. 843-858.
- Coplen, T.B., and Hanshaw, B.D., 1973, Ultrafiltration by a compacted clay membrane-I. Oxygen and hydrogen isotopic fractionation: *Geochimica et Cosmochimica Acta*, v. 37, p. 2295-2310.
- Craig, H., 1969, Geochemistry and origin of the Red Sea brines, in Degens, E.T., and Ross, D.A., eds., *Hot brines and recent heavy metal deposits in the Red Sea*: New York, Springer-Verlag, p. 208-242.
- Craig, H., and Gordon, L.I., 1965, Deuterium and oxygen 18 variations in the ocean and marine atmosphere, in Tongiorgi, E., ed., *Stable isotopes in oceanographic studies and paleotemperatures*: Pisa, Italy, Consiglio Nazionale delle Ricerche, Laboratorio di Geologia Nucleare, p. 9-130.
- Crerar, D., Wood, S., Brantley, S., and Bocarsly, A., 1985, Chemical controls on solubility of ore-forming minerals in hydrothermal solutions: *Canadian Mineralogist*, v. 23, p. 333-352.
- Cullers, R.L., Chaudhuri, S., Kilbane, N., and Koch, R., 1979, Rare earths in size fractions and sedimentary rocks of Pennsylvanian age from the mid-continent of the U.S.A.: *Geochimica et Cosmochimica Acta*, v. 37, p. 1499-1512.
- Dawson, K., 1990, Regional geologic setting of selected mineral deposits of the Northern Cordillera, in Abbott, J.G., and Turner, R.W.J., eds., *Mineral deposits of the Northern Canadian Cordillera, Yukon-Northeastern British Columbia (Field Trip 14)*: 8th IAGOD Symposium Field Trip Guidebook: Geological Survey of Canada Open File 2169, p. 1-24.
- Deer, W.A., Howie, R.A., and Zussman, J., 1966, *An introduction to the rock forming minerals*: London, Longman.
- de Ronde, C.E.J., 1995, Fluid chemistry and isotopic characteristics of seafloor hydrothermal systems and associated VMS deposits: potential for magmatic contributions, in Thompson, J.F.H., ed., *Magma, fluids and ore deposits*: Mineralogical Association of Canada Short Course Series, v. 23, p. 479-510.
- Deuser, W.G., 1970, Carbon-13 in Black Sea waters and implications for the origin of hydrogen sulfide: *Science*, v. 168, p. 1575-1577.
- Devol, A.H., Anderson, J.J., Kuivila, K., and Murray, J.W., 1984, A model for coupled sulfate reduction and methane oxidation in the sediments of Saanich Inlet: *Geochimica et Cosmochimica Acta*, v. 48, p. 993-1004.
- Duckworth, R.C., Fallick, A.E., and Rickard, D., 1994, Mineralogy and sulfur isotopic composition of the Middle Valley massive sulfide deposit: northern Juan de Fuca Ridge, in Mottl, M.J., Davis, E.E., Fisher, A.T. and Slack, J.F., eds., *Proceedings of the Ocean Drilling Program: College Station, Texas, Ocean Drilling Program, Scientific Results*, v. 130, p. 373-385.
- Dymond, J., Corliss, J.B., and Heath, G.R., 1977, History of metalliferous sedimentation at Deep Sea Drilling Site 319, in the south east Pacific: *Geochimica et Cosmochimica Acta*, v. 41, p. 741-753.
- Eldridge, C.S., Barton, P.B., Jr., and Ohmoto, H., 1983, Mineral textures and their bearing on formation of the Kuroko orebodies: *Economic Geology Monograph* 5, p. 241-281.
- Forbes, R.B., 1986, A preliminary report on the geologic setting and petrology of the metavolcanic rocks in the northwestern part of the Skagway B-4 Quadrangle, southeastern Alaska: U.S. Bureau of Mines unpublished report, 27 p.
- Fournier, R.O., 1985, The behavior of silica in hydrothermal solutions, in Berger, B.R., and Bethke, P.M., eds., *Geology and geochemistry of epithermal systems: Reviews in Economic Geology*, v. 2, p. 45-61.
- Fryer, P., Sinton, J.M., and Philpotts, J.A., 1981, Basaltic glasses from the Mariana Trough: Initial Reports of the Deep Sea Drilling Project, v. 60, p. 601-609.
- Gammon, J.B., and Chandler, T.E., 1986, Exploration of the Windy Craggy massive sulphide deposit, British Columbia, in geology in the real world—The Kingsley Dunham volume: London, The Institution of Mining and Metallurgy, p. 131-141.
- Gardner, M.C., Bergman, S.C., Cushing, G.W., Mackevett, E.M., J. Plafker, G., Campbell, R.E., Dodd, C.J., McClelland, W.C., and Muelle, P.A., 1988, Pennsylvanian pluton stitching of Wrangellia and the Alexander terrane, Wrangell Mountains, Alaska: *Geology*, v. 16, p. 967-971.
- Gasparrini, C., 1983, Study of the gold, silver, and cobalt distribution in two samples of core from the Windy Craggy deposit: Geddes Resources Ltd., unpublished proprietary report.
- Geddes Resource Ltd. 1991: Third quarter report to shareholders, November 18, 1991, 6 p.
- Gehrels, G.E., 1990, Late Proterozoic-Cambrian metamorphic basement of the Alexander terrane on Long and Dall Islands, southeast Alaska: *Geological Society of America Bulletin*, v. 102, p. 760-767.
- Gerlach, T.M., and Taylor, B.E., 1990, Carbon isotope constraints on degassing of carbon dioxide from Kilauea Volcano: *Geochimica et Cosmochimica Acta*, v. 54, p. 2051-2058.
- Goldhaber, M.B., and Kaplan, I.R., 1975, Controls and consequences of sulfate reduction rates in marine sediments: *Soil Science*, v. 119, p. 42-55.
- Grant, J.A., 1986, The Isocon Diagram—a simple solution to Gresens's equation for metasomatic alteration: *Economic Geology*, v. 81, p. 1976-1987.
- Green, D.H., 1973, Conditions of melting of basanite magma from garnet peridotite: *Earth and Planetary Science Letters*, v. 17, p. 456-465.
- Grenne, T., and Vokes, F.M., 1990, Sea-floor sulfides at the Hoydal volcanicogenic deposit, central Norwegian Caledonides: *Economic Geology*, v. 85, p. 344-359.
- Gresens, R.L., 1967, Composition-volume relationships of metasomatites: *Chemical Geology*, v. 2, p. 47-65.
- Gromet, L.P., Dymek, R.F., Haskin, L.A., and Korotev, R.L., 1984, The "North American shale composite": Its compilation, major and trace element characteristics: *Geochimica et Cosmochimica Acta*, v. 48, p. 2469-2482.
- Harris, J.F., 1988, Petrographic study of rocks from the Windy Craggy area, Atlin Mining District, B.C.: Geddes Resources Ltd., unpublished proprietary report.
- Hofmann, A.W., 1997, Mantle geochemistry: The message from ocean volcanism: *Nature*, v. 385, p. 219-229.
- Hogdahl, O.T., Melson, S., and Bowen, V.T., 1968, Neutron activation analysis of lanthanide elements in seawater, in Gould, R.F., ed., *Trace inorganics in water: Advances in chemistry series*, v. 73, p. 308-325.
- Horikoshi, E., 1959, Colloform textures of cupriferous pyrite ores in the Okuki and Nebutoyama mines: *Mining Geol.*, v. 9, p. 82-94.
- Hudson, J.D., 1977, Stable isotopes and limestone lithification: *Journal of the Geological Society, London*, v. 133, p. 637-660.
- Humphris, S.E., Herzig, P.M., and Miller, D.J. (eds.), 1995, *Proceedings of the Ocean Drilling Program, Initial Reports*: College Station, Texas: Ocean Drilling Program, v.158, 384 p.

- Irvine, T.N., and Baragar, W.R.A., 1971, A guide to the chemical classification of the common volcanic rocks: *Canadian Journal of Earth Sciences*, v. 8, p. 523-548.
- Itoh, S., 1976, Geochemical study of bedded cupriferous pyrite deposits in Japan: *Bulletin of the Geological Survey of Japan*, v. 27, p. 245-377.
- Johnson, K.T.M., and Sinton, J.M., 1990, Petrology, tectonic setting and the formation of back-arc basin basalts in the North Fiji Basin: *Geologisches Jahrbuch*, v. D92, p. 517-545.
- Kalogeropoulos, S.I., and Scott, S.D., 1983, Mineralogy and geochemistry of tuffaceous exhalites (Tetsusekiei) of the Fukazawa mine, Hokuroku district, Japan: *Economic Geology Monograph* 5, p. 412-432.
- Karhu, J., and Epstein, S., 1986, The implication of the oxygen isotope records in coexisting cherts and phosphates: *Geochimica et Cosmochimica Acta*, v. 50, p. 1745-1756.
- Kase, K., and Yamamoto, M., 1988, Minerals and geochemical characteristics of ores from the Besshi-type deposits in the Sanbagawa belt, Japan: *Mining Geology*, v. 38, p. 203-214.
- Kelemen, P.B., and Radford, G.W., 1983, Geology of the north face of Windy Peak, Windy Craggy copper deposit: Falconbridge Ltd., unpublished proprietary report.
- Kharaka, Y.K., Berry, F.A.F., and Friedman, I., 1973, Isotopic composition of oil-field brines from Kettleman North Dome oil field, California, and their geologic implications: *Geochimica et Cosmochimica Acta*, v. 37, p. 1899-1908.
- Kissin, S.A., 1974, Phase Relations in a Portion of the Fe-S System: Unpublished Ph.D. thesis, Toronto, University of Toronto.
- Klein, G., 1975a, Depositional facies of leg 30 DSDP sediment cores, in Andrews, J.E., Packham, G., et al., eds., *Initial Reports of the Deep Sea Drilling Project*, Washington, D.C., U.S. Government Printing Office, v. 30, p. 423-442.
- 1975b, Sedimentary tectonics in Southwest Pacific marginal basins based on Leg 30 Deep Sea Drilling Project cores from the South Fiji, Hebrides, and Coral Sea Basins: *Geological Society of America Bulletin*, v. 86, p. 1012-1018.
- Large, R.R., 1977, Chemical evolution and zonation of massive sulfide deposits in volcanic terrains: *Economic Geology*, v. 72, p. 549-572.
- Le Bel, L., and Oudin, E., 1982, Fluid inclusion studies of deep-sea hydrothermal sulphide deposits on the East Pacific Rise near 21°N: *Chemical Geology*, v. 37, p. 129-136.
- Lowell, R.P., and Rona, P.A., 1985, Hydrothermal models for the generation of massive sulfide ore deposits: *Journal of Geophysical Research*, v. 90, p. 8769-8783.
- MacIntyre, D.G., 1983, A comparison of stratiform massive sulphide deposits of the Gataga District with the Midway and Windy Craggy deposits, northern British Columbia, *Geological Fieldwork 1982*: B.C. Ministry of Energy, Mines and Petroleum Resources Paper 1983-1, p. 149-170.
- 1984, Geology of the Alsek-Tatshenshini Rivers area (114P), *Geological Fieldwork 1983*: B.C. Ministry of Energy, Mines and Petroleum Resources Paper 1984-1, p. 173-184.
- 1986, The geochemistry of basalts hosting massive sulphide deposits, Alexander Terrane, northwest British Columbia, *Geological Fieldwork 1985*: B.C. Ministry of Energy, Mines, and Petroleum Resources, Paper 1987-1, p. 197-210.
- Maeda, H., Ito, Y., Aragane, T., and Sato, J., 1981, Modes of occurrence and properties of electrum from the Shimokawa cupriferous iron sulphide deposits—in comparison with those from the Kuroko deposits: *Mining Geology*, v. 10, p. 193-202.
- Mainwaring, P.R., 1983, Initial mineralogical characterization of the Windy Craggy Cu-Co deposit, British Columbia, CANMET, unpublished report.
- McCarthy, P., and Robinson, M., 1991, Tectonics and mineralogy: Windy Craggy massive sulphide deposit, northwestern British Columbia, University of British Columbia, unpublished mineralogy course report.
- McLennan, S.M., Taylor, S.R., McCulloch, M.T., and Maynard, J.B., 1990, Geochemical and Nd-Sr isotopic composition of deep-sea turbidites: Crustal evolution and plate tectonic associations: *Geochimica et Cosmochimica Acta*, v. 54, p. 2015-2050.
- Menzies, M., and Seyfried, W.E., Jr., 1979, Basalt-seawater interaction: Trace element and strontium isotopic variations in experimentally altered glassy basalt: *Earth and Planetary Science Letters*, v. 44, p. 463-472.
- Meschede, M., 1986, A method of discriminating between different types of mid-ocean ridge basalts and continental tholeiites with the Nb-Zr-Y diagram: *Chemical Geology*, v. 56, p. 207-218.
- Michard, A., and Albarede, F., 1986, The REE content of some hydrothermal fluids: *Chemical Geology*, v. 55, p. 51-60.
- Mihalynuk, M.G., Smith, M.T., MacIntyre, D.G., and Deschênes, M., 1993, Tatshenshini project, northwestern British Columbia. Part B: Stratigraphic and magmatic setting of mineral occurrences, *Geological Fieldwork 1992*: Victoria, B.C.: B.C. Ministry of Energy, Mines and Petroleum Resources, Paper 1993-1, p. 189-202.
- Monger, J.W.H., Price, R.A., and Tempelman-Kluit, D.J., 1982, Tectonic accretion and the origin of the two major metamorphic and plutonic belts in the Canadian Cordillera: *Geology*, v. 10, p. 70-75.
- Mottl, M.J., 1983, Metabasalts, axial hot springs, and the structure of hydrothermal systems at mid-ocean ridges: *Geological Society of America Bulletin*, v. 94, p. 161-180.
- Mottl, M.J., and Holland, H.D., 1978, Chemical exchange during hydrothermal alteration of basalt by seawater—I. Experimental results for major and minor components of seawater: *Geochimica et Cosmochimica Acta*, v. 42, p. 1103-1115.
- Mottl, M.J., and McConachy, T.F., 1990, Chemical processes in buoyant hydrothermal plumes on the East Pacific Rise near 21°N: *Geochimica et Cosmochimica Acta*, v. 54, p. 1911-1927.
- Mottl, M.J., Holland, H.D., and Corr, R.F., 1979, Chemical exchange during hydrothermal alteration of basalt by seawater—II. Experimental results for Fe, Mn, and sulfur species: *Geochimica et Cosmochimica Acta*, v. 43, p. 869-884.
- Mottl, M.J., Davis, E.E., Fisher, A.T., et al., eds., 1994, *Proceedings of the Ocean Drilling Program, Scientific Results*: College Station, Texas, Ocean Drilling Program, v. 139, 772 p.
- Muir, J.E., 1980, Mineralogical examination of a suite of mineralized samples from the area of the Alsek (Windy Craggy) copper deposit, northwestern B.C.: Falconbridge Metallurgical Laboratories, unpublished report MR-1139.
- Norford, B.S., and Mihalynuk, M.G., 1994, Evidence of the Pacific Faunal Province in the northern Alexander Terrane, recognition of two Middle Ordovician graptolite zones in northwestern British Columbia: *Canadian Journal of Earth Sciences*, v. 31, p. 1389-1396.
- Northern Miner, 1983, Big gold intersection is pulled on B.C. Windy Craggy copper bet, October 13, 1983: Toronto, p. 1.
- 1988, Windy Craggy encourages Geddes, May 9, 1988: Toronto, p. 13.
- Orchard, M.J., 1986, Conodonts from western Canadian chert: Their nature, distribution and stratigraphic application, in Austin, R.L., ed., *Conodonts: Investigative techniques and applications*: Chichester, England, Ellis Horwood Ltd., p. 94-119.
- Oudin, E., 1983, Hydrothermal sulfide deposits of the East Pacific Rise (21°N) Part 1: Descriptive mineralogy: *Marine Mining*, v. 4, p. 39-72.
- Palmer, M.R., 1985, Rare earth elements in foraminifera tests: *Earth and Planetary Science Letters*, v. 73, p. 285-298.
- Parekh, P.P., Moller, P., Dulski, P., and Bausch, W.M., 1977, Distribution of trace elements between carbonates and non-carbonate phases of limestone: *Earth and Planetary Science Letters*, v. 34, p. 39-50.
- Pearce, J.A., 1983, Role of sub-continental lithosphere in magma genesis at destructive plate margins, in Hawkesworth, C.J., and Norry, M.J., eds., *Continental basalts and mantle xenoliths*: Nantwich, Shiva, p. 230-249.
- Peter, J.M., 1989, The Windy Craggy copper-cobalt-gold massive sulphide deposit, northwestern British Columbia: in: *British Columbia Ministry of Energy, Mines and Petroleum Resources, Geological Fieldwork 1988*, Paper 1989-1, p. 455-466.
- 1992, Comparative geochemical studies of the Upper Triassic Windy Craggy and modern Guaymas Basin deposits: A contribution to the understanding of massive sulfide formation in volcano-sedimentary environments: Unpublished Ph.D. thesis, Toronto, University of Toronto, 562 p.
- Peter, J.M., and Scott, S.D., 1988, Mineralogy, composition, and fluid-inclusion microthermometry of seafloor hydrothermal deposits in the southern trough of Guaymas basin, Gulf of California: *Canadian Mineralogist*, v. 26, p. 567-587.
- 1990, Mineralogy and geochemistry of the Windy Craggy copper-cobalt-gold massive sulphide deposit, northwestern British Columbia, Canada, in Abbott, J.G., and Turner, R.W.J., eds., *Mineral deposits of*

- the Northern Canadian Cordillera, Yukon—Northeastern British Columbia (Field Trip 14): 8th IAGOD Symposium Field Trip Guidebook, Geological Survey of Canada Open File 2169, p. 31–67.
- 1993, Fluid inclusion and light stable isotope geochemistry of the Windy Craggy Besshi-type massive sulfide deposit, northwestern British Columbia: *Resource Geology Special Issue*, v. 17, p. 229–248.
- Piper, D.Z., and Graef, P.A., 1974, Gold and rare-earth elements in sediments from the East Pacific Rise: *Marine Geology*, v. 17, p. 287–297.
- Pisutha-Arnond, V., and Ohmoto, H., 1983, Thermal history, and chemical and isotopic compositions of the ore-forming fluids responsible for the Kuroko massive sulfide deposits in the Hokuroku district of Japan: *Economic Geology Monograph* 5, p. 523–558.
- Potter, R.W., 1977, Pressure corrections for fluid-inclusion homogenization temperatures based on the volumetric properties of the system NaCl-H₂O: *Journal of Research of the U.S. Geological Survey*, v. 5, p. 603–607.
- Price, R.C., Johnson, L.E., and Crawford, A.J., 1990, Basalts of the North Fiji Basin: The generation of back arc basin magmas by mixing of depleted and enriched mantle sources: *Contributions to Mineralogy and Petrology*, v. 105, p. 106–121.
- Prince, D.R., 1983, Report on reconnaissance geological mapping of the Windy Craggy area, B.C., NTS 114P: Falconbridge Ltd., unpublished report.
- Ramboz, C., Oudin, E., and Thisse, Y., 1988, Geyser-type discharge in Atlantis II Deep, Red Sea: Evidence of boiling from fluid inclusions in epigenetic anhydrite: *Canadian Mineralogist*, v. 26, p. 765–786.
- Ramsay, J.G., 1980, The crack-seal mechanism of rock deformation: *Nature*, v. 284, p. 135–139.
- Robertson, A.H.F., and Hudson, J.D., 1973, Cyprus umbers: Chemical precipitates on a Tethyan ocean ridge: *Earth and Planetary Science Letters*, v. 18, p. 93–101.
- Rock, N.M.S., 1988, The need for standardization of normalized multi-element diagrams in geochemistry: A comment: *Geochemical Journal*, v. 21, p. 75–84.
- Roedder, E., 1981, Natural occurrence and significance of fluids indicating high pressure and temperature, in Rickard, D.T., and Wickman, F.E., eds., *Chemistry and geochemistry of Solutions at high temperature*: Oxford, Pergamon Press, p. 9–39.
- Roedder, E., and Bodnar, R.J., 1980, Geologic pressure determinations from fluid inclusion studies: *Annual Review of Earth and Planetary Sciences*, v. 8, p. 263–301.
- Sakai, H.D., Des Marais, D.J., Ueda, A., and Moore, J.C., 1984, Concentrations and isotope ratios of carbon, nitrogen, and sulfur in ocean-floor basalts: *Geochimica et Cosmochimica Acta*, v. 48, p. 2433–2441.
- Samson, S.D., and Patchett, P.J., 1991, The Canadian Cordillera as a modern analogue of Proterozoic crustal growth: *Australian Journal of Earth Sciences*, v. 38, p. 595–611.
- Samson, S.D., McClelland, W.C., Patchett, P.J., Gehrels, G.E., and Anderson, R.G., 1989, Evidence from neodymium isotopes for mantle contributions to Phanerozoic crustal genesis in the Canadian Cordillera: *Nature*, v. 337, p. 705–709.
- Saunders, A.D., Tarney, J., Stern, C.R., and Dalziel, I.W.D., 1979, Geochemistry of Mesozoic marginal basin floor igneous rocks from southern Chile: *Geological Society of America Bulletin*, v. 90, p. 237–258.
- Savin, S.M., and Epstein, S., 1970a, The oxygen and hydrogen isotope geochemistry of clay minerals: *Geochimica et Cosmochimica Acta*, v. 34, p. 25–42.
- 1970b, The oxygen and hydrogen isotope geochemistry of ocean sediments and shales: *Geochimica et Cosmochimica Acta*, v. 34, p. 43–63.
- Schilling, J.G., Zajac, M., Evans, R., Johnston, T., White, T., Devine, W., and Kingsley, R., 1983, Petrologic and geochemical variations along Mid-Atlantic Ridges from 29°N to 73°N: *American Journal of Science*, v. 283, p. 510–586.
- Seyfried, W.E., Jr., and Bischoff, J.L., 1977, Hydrothermal transport of heavy metals by seawater: The role of seawater/basalt ratio: *Earth and Planetary Science Letters*, v. 34, p. 71–77.
- 1979, Low temperature basalt alteration by seawater: An experimental study at 70°C and 150°C: *Geochimica et Cosmochimica Acta*, v. 43, p. 1937–1947.
- Seyfried, W.E., Jr., and Mottl, M.J., 1982, Hydrothermal alteration of basalt by seawater under seawater-dominated conditions: *Geochimica et Cosmochimica Acta*, v. 46, p. 985–1002.
- Seyfried, W.E., Jr., Berndt, M.E., and Janecky, D.R., 1986, Chloride depletions and enrichments in seafloor hydrothermal fluids: Constraints from experimental basalt alteration studies: *Geochimica et Cosmochimica Acta*, v. 50, p. 469–475.
- Shanks, W.C., III, Bischoff, J.L., and Rosenbauer, R.J., 1981, Seawater sulfate reduction and sulfur isotope fractionation in basaltic systems: interaction of seawater with fayalite and magnetite at 200–350°C: *Geochimica et Cosmochimica Acta*, v. 45, p. 1977–1996.
- Shanks, W.C., III, Böhlke, J.K., and Seal, R.R., II., 1995, Stable isotopes in mid-ocean ridge hydrothermal systems: interactions between fluids, minerals, and organisms, in seafloor hydrothermal systems: Physical, chemical, biological, and geological interactions: *American Geophysical Union, Monograph* 91, p. 194–221.
- Shaw, H.F., and Wasserburg, G.J., 1985, Sm-Nd in marine carbonates and phosphates: implications for Nd isotopes in seawater and crustal ages: *Geochimica et Cosmochimica Acta*, v. 49, p. 503–518.
- Sheppard, S.M.F., 1986, Characterization and isotopic variations in natural waters, in Valley, J.W., Taylor, H.P., Jr., and O'Neil, J.R., eds., *Stable isotopes in high temperature geological processes: Reviews in Mineralogy*, Mineralogical Society of America, Washington, D.C., v. 16, p. 165–183.
- Shibata, T., Thompson, G., and Frey, F.A., 1979, Tholeiitic and alkali basalts from the Mid-Atlantic Ridge at 43°N: *Contributions to Mineralogy and Petrology*, v. 70, p. 127–141.
- Shimizu, H., and Masuda, A., 1977, Cerium in chert as an indicator of marine environment of its formation: *Nature*, v. 266, p. 346–348.
- Sinton, J.M., and Fryer, P., 1987, Mariana Trough lavas from 18°N: Implications for the origin of back arc basin basalts: *Journal of Geophysical Research*, v. 92, p. 12782–12802.
- Slack, J.F., 1993, Descriptive and grade-tonnage models for Besshi-type massive sulphide deposits, in Kirkham, R.V., Sinclair, W.D., Thorpe, R.I., and Duke, J.M., eds., *Mineral deposit modeling*, Geological Association of Canada, Special Paper 40, p. 343–371.
- Smith, A.D., and Fox, J.S., 1989a, Geochemistry of basalts from the Windy Craggy and Anyox volcanogenic massive sulphide deposits, British Columbia [abs.]: in *Geological Association of Canada/Mineralogical Association of Canada Program with Abstracts*, v. 14, p. A22.
- 1989b, Geochemistry of Upper Triassic basalts from the Anyox and Windy Craggy volcanogenic massive sulphide deposits, British Columbia: unpublished manuscript.
- Smith, M.T., Mihalynuk, M.G., and MacIntyre, D.G., 1993, Tatshenshini project, northwestern British Columbia. Part C: Deformation and structural styles: B.C. Ministry of Energy, Mines and Petroleum Resources, *Geological Fieldwork 1992, Paper 1993-1*, p. 203–216.
- Stacey, J.S., and Kramers, J.D., 1975, Approximation of terrestrial lead isotope evolution by a two-stage model: *Earth and Planetary Science Letters*, v. 26, p. 207–221.
- Stebbins, J., and Thompson, G., 1978, The nature and petrogenesis of intra-ocean plate alkaline eruptive and plutonic rocks: King's Trough north-east Atlantic: *Journal of Volcanological and Geothermal Research*, v. 4, p. 333–361.
- Stiller, M., Rounick, J.S., and Shasha, S., 1985, Extreme carbon-isotope enrichments in evaporating brines: *Nature*, v. 316, p. 434–435.
- Sun, S.-S., 1980, Lead isotope study of young volcanic rocks from mid-ocean ridges, ocean islands and island arcs: *Philosophical Transactions of the Royal Society of London*, v. A297, p. 409–445.
- Sun, S.-S., Nesbitt, R.W., and Sharaskin, A.Y., 1979, Geochemical characteristics of mid-ocean ridge basalts: *Earth and Planetary Science Letters*, v. 44, p. 119–138.
- Sverjensky, D.A., 1984, Europium redox equilibria in aqueous solution: *Earth and Planetary Science Letters*, v. 67, p. 70–78.
- Takeda, H., and Sekine, Y., 1960, A consideration of the metamorphism of cupriferous pyritic deposit at Sekizen, Ehime Prefecture: *Mining Geology*, v. 10, p. 369–379.
- Tarney, J., Wood, D.A., Saunders, A.D., Cann, J.R., and Varet, J., 1980, Nature of mantle heterogeneity in the North Atlantic: Evidence from deep sea drilling: *Philosophical Transactions of the Royal Society of London*, v. 297A, p. 179–202.
- Taylor, H.P., Jr., 1980, The effects of assimilation of country rocks by magmas on ¹⁸O/¹⁶O and ⁸⁷Sr/⁸⁶Sr systematics in igneous rocks: *Earth and Planetary Science Letters*, v. 47, p. 243–254.

- Taylor, S.R., and McLennan, S.M., 1985, The continental crust: its composition and evolution: Oxford, Blackwell Scientific Publications, 312 p.
- Thornton, E.C., and Seyfried, W.E., Jr., 1987, Reactivity of organic-rich sediment in seawater at 350°C, 500 bars: Experimental and theoretical constraints and implications for the Guaymas Basin hydrothermal system: *Geochimica et Cosmochimica Acta*, v. 51, p. 1997-2010.
- Tsunori, T., 1962, Microscopical study of ores from cupriferous iron sulfide deposits in Shikoku, Japan: Sumitomo Metal Mining Co. Ltd., unpublished technical report.
- Turner, J.S., and Campbell, I.H., 1987, Temperature, density and buoyancy fluxes in "black smoker" plumes, and the criterion for buoyancy reversal: *Earth and Planetary Science Letters*, v. 86, p. 85-92.
- Urabe, T., and Marumo, K., 1991, A new model for Kuroko-type deposits of Japan: *Episodes*, v. 14, p. 246-268.
- Urabe, T., and Scott, S.D., 1983, Geology and footwall alteration of the South Bay massive sulphide deposit, northwestern Ontario, Canada: *Canadian Journal of Earth Sciences*, v. 20, p. 1862-1879.
- Van der Voo, R., Jones, M., Gromme, C.S., Iberlein, G.D., and Churkin, M.J., 1980, Paleozoic paleomagnetism and the northward drift of the Alexander terrane, southeastern Alaska: *Journal of Geophysical Research*, v. 85, p. 5281-5296.
- Veizer, J., and Hoefs, J., 1976, The nature of O^{18}/O^{16} and C^{13}/C^{12} secular trends in sedimentary carbonate rocks: *Geochimica et Cosmochimica Acta*, v. 40, p. 1387-1395.
- Von Damm, K.L., 1990, Seafloor hydrothermal activity: Black smoker chemistry and chimneys: *Annual Review of Earth and Planetary Sciences*, v. 18, p. 173-204.
- Weaver, S.D., Saunders, A.D., Pankhurst, R.J., and Tarney, J., 1979, A geochemical study of magmatism associated with the initial stages of back-arc spreading: *Contributions to Mineralogy and Petrology*, v. 68, p. 151-169.
- Wheeler, J.O., and McFeely, P., 1991, Tectonic assemblage map of the Canadian Cordillera: Geological Survey of Canada Map 1712A, scale 1:2,000,000.
- Winchester, J.A., and Floyd, P.A., 1977, Geochemical discrimination of different magma series and their differentiation products using immobile elements: *Chemical Geology*, v. 20, p. 325-343.
- Wood, D.A., 1980, The application of a Th-Hf-Ta diagram to problems of tectonomagmatic classification and to establishing the nature of crustal contamination of basaltic lavas of the British Tertiary volcanic province: *Earth and Planetary Science Letters*, v. 50, p. 11-30.
- Wright, T.L., 1984, Origin of Hawaiian tholeiite: A metasomatic model: *Journal of Geophysical Research*, v. 89, p. 3233-3252.
- Zierenberg, R.A., Koski, R.A., Morton, J.L., Bouse, R.M., and Shanks, W.C., III, 1993, Genesis of massive sulfide deposits on a sediment-covered spreading center, Escanaba trough, southern Gorda Ridge: *Economic Geology*, v. 88, p. 2037-2068.